

000  
001  
002  
003  
004  
005  
006  
007  
008  
009  
010  
011  
012  
013  
014  
015  
016  
017  
018  
019  
020  
021  
022  
023  
024  
025  
026  
027  
028  
029  
030  
031  
032  
033  
034  
035  
036  
037  
038  
039  
040  
041  
042  
043  
044  
045  
046  
047  
048  
049  
050  
051  
052  
053  

# UNDERSTANDING TOOL-INTEGRATED REASONING

**Anonymous authors**

Paper under double-blind review

## ABSTRACT

We study why Tool-Integrated Reasoning (TIR) makes Large Language Models (LLMs) more capable. While LLMs integrated with tools like Python code interpreters show great promise, a principled theory explaining why this paradigm is effective has been missing. This work provides the first formal proof that TIR fundamentally expands an LLM’s capabilities. We demonstrate that tools enable a strict expansion of the model’s empirical and feasible support, breaking the capability ceiling of pure-text models by unlocking problem-solving strategies that are otherwise impossible or intractably verbose. To guide model behavior without compromising training stability and performance, we also introduce Advantage Shaping Policy Optimization (ASPO), a novel algorithm that directly modifies the advantage function to guide the policy behavior. We conduct comprehensive experiments on challenging mathematical benchmarks, leveraging a Python interpreter as the external tool. Our results show that the TIR model decisively outperforms its pure-text counterpart on the  $\text{pass}@k$  metric. Crucially, this advantage is not confined to computationally-intensive problems but extends to those requiring significant abstract insight. We further identify the emergent cognitive patterns that illustrate how models learn to *think with tools*. Finally, we report improved tool usage behavior with early code invocation and much more interactive turns with ASPO. Overall, our work provides the first principled explanation for TIR’s success, shifting the focus from the mere fact *that tools work* to *why* and *how* they enable more powerful reasoning.

## 1 INTRODUCTION

Large language models (LLMs) have rapidly progressed from fluent generators to general-purpose problem solvers. Nevertheless, purely text-based reasoning often struggles with tasks that demand precise calculation, long-horizon search, faithful verification, or access to information beyond a model’s parametric memory. As a powerful and empirically successful paradigm, Tool-Integrated Reasoning (TIR) (Feng et al., 2025; Li et al., 2025b) has emerged to address these limitations. Systems equipped with external tools have consistently and significantly outperformed their pure-text counterparts (OpenAI, 2025a;b; xAI, 2025). However, despite the widespread recognition of TIR’s effectiveness, a principled account of the fundamental mechanisms, specifically *why* and *when* it helps, is still missing. Existing research has largely focused on demonstrating empirical success, leaving a crucial gap for a formal framework that can elucidate the origins of its benefits and define its capability boundaries.

To build such a framework, we first turn to reinforcement learning (RL) (Lambert et al., 2024; Sutton et al., 1998), the predominant paradigm for enhancing LLM reasoning. Recent theoretical work has established a critical consensus: in a pure-text environment, RL is constrained by an “invisible leash” (Wu et al., 2025). The learning process is largely confined to re-weighting probabilities within the base model’s pre-existing trajectories, meaning it cannot discover fundamentally new reasoning trajectories that lie outside this initial capability (Yue et al., 2025).

The central thesis of this work is that tool integration fundamentally breaks this barrier. By introducing deterministic, non-linguistic state transitions via an external tool like a Python interpreter, TIR fundamentally expands the model’s exploratory space. We provide the first formal proof that TIR enables a *strict expansion* of the model’s empirical support, allowing it to generate correct trajectories that have negligible or even zero probability in a pure-text paradigm. Beyond theoretical reachability, we introduce the concept of *token efficiency* to argue that tools are a practical necessity. For any finite

054 token budget, there exist algorithmic strategies whose programmatic representations are concise,  
 055 while their natural-language simulations are intractably verbose. Consequently, TIR unlocks a vastly  
 056 larger *feasible support* of problem-solving strategies that are simply out of reach for pure-text models  
 057 under realistic constraints. Extensions to other tools with informal propositions can be found in  
 058 Appendix E.

059 We validate these theoretical claims through a series of experiments focusing on solving mathematical  
 060 competition problems with a Python code interpreter. Our  $\text{pass}@k$  analysis provides clear evidence  
 061 that TIR decisively breaks the capability ceiling of pure-text models. Further investigation, using  
 062 our proposed “algorithmic friendliness” metric, reveals that TIR’s benefits are not confined to  
 063 computationally-intensive problems but extend to those requiring significant abstract insight. Case  
 064 studies of the model’s behavior further illuminate *how* it leverages this expanded capability, revealing  
 065 three emergent cognitive patterns: insight-to-computation transformation, exploration & verification  
 066 via code, and offloading of complex calculations.

067 Finally, in exploring how to further optimize TIR models, we identify a practical algorithmic challenge:  
 068 guiding model behavior, such as encouraging earlier tool use, via traditional reward shaping often  
 069 leads to training instability in GRPO-like algorithms (Shao et al., 2024; Feng et al., 2025). To address  
 070 this, we propose Advantage Shaping Policy Optimization (**ASPO**), a novel algorithm that circumvents  
 071 the reward function and instead applies a stable, controllable bias directly to the advantage function.  
 072 Our experiments show that ASPO successfully guides model behavior with early tool invocation and  
 073 increased tool usages without compromising task performance or training stability.

074 Our contributions are as follows:

- 076 1. We provide the first formal theory for why TIR expands an LLM’s capabilities, proving that  
 077 it enables a strict expansion of both the feasible and empirical support compared to pure-text  
 078 models.
- 079 2. We propose Advantage Shaping Policy Optimization (**ASPO**), a novel and stable algo-  
 080 rithm for guiding the behavior of TIR models by directly shaping the advantage function,  
 081 overcoming the instability of traditional reward-based methods.
- 082 3. We conduct a comprehensive empirical analysis that not only validates our theoretical claims  
 083 and algorithm but also provides a mechanistic explanation of TIR’s effectiveness, identifying  
 084 its universal benefits across problem types and the emergent cognitive patterns it fosters.

## 086 2 RELATED WORK

088 A significant body of work focuses on developing RL frameworks for strategic tool use. Feng et al.  
 089 (2025) propose ReTool, an RL-based framework that demonstrates high data efficiency for learning  
 090 tool use. Similarly, Li et al. (2025b) introduce ToRL, a method designed to address the challenges of  
 091 scaling tool-integrated RL to more complex and demanding scenarios. Bai et al. (2025) document  
 092 methods for effective code-integrated reasoning. This paradigm shares the goal of augmenting LLM  
 093 reasoning with external Python execution. Focusing on training from base models, Xue et al. (2025)  
 094 present SimpleTIR, an end-to-end framework for multi-turn TIR that enables stable training from  
 095 scratch, a process they refer to as the “Zero” setting.

096 **Beyond these RL-for-tool frameworks, other research investigates the limitations of RL for pure-text**  
 097 **reasoning.** Yue et al. (2025) empirically find that RL does not incentivize novel reasoning capacity.  
 098 Providing a theoretical framework to explain such findings, Wu et al. (2025) propose the “invisible  
 099 leash” theory, suggesting that models may struggle to discover reasoning paths outside their original  
 100 knowledge distribution.

101 Beyond programmatic tools like Python interpreters, another line of work integrates search engines  
 102 to equip LLMs with up-to-date knowledge via RL. Jin et al. (2025) propose Search-R1, where LLMs  
 103 interleave reasoning with real-time queries, trained with outcome-based rewards and stabilized by  
 104 masking retrieved tokens, achieving strong multi-turn QA performance. To tackle uncertainty in  
 105 complex web tasks, Li et al. (2025a) introduce WebSailor, a post-training method that narrows the  
 106 gap with proprietary agents. In this work, we primarily focus on utilizing Python interpreters to  
 107 enhance the LLM’s ability to solve complex reasoning problems in mathematics; similar principles  
 apply for enhancing knowledge-seeking ability and we have informal discussions in Appendix E.

108 

### 3 METHOD

110 In this section, we formalize the argument that integrating an external computational tool, such as a  
 111 code interpreter, fundamentally enhances a Large Language Model’s (LLM) capabilities. We structure  
 112 our argument in two parts. First, we provide a formal proof demonstrating that tool integration results  
 113 in a strict expansion of the model’s generative support, thereby breaking the “invisible leash” that  
 114 constrains purely text-based models (Wu et al., 2025). Second, we introduce the concept of *token*  
 115 *efficiency* to argue that even for problems theoretically solvable by text-based models, tool integration  
 116 is a practical necessity for expressing complex algorithms within any feasible token budget. **It is**  
 117 **worth emphasizing that our aim here is not to obtain surprising complexity-theoretic separations, but**  
 118 **to introduce a precise vocabulary and analytical lens missing in prior work, which enables systematic**  
 119 **reasoning about tool-augmented models.**

120 

#### 3.1 FORMAL PROOF: SUPPORT EXPANSION VIA TOOL INTEGRATION

121 We begin by establishing that augmenting an LLM with a deterministic external tool strictly expands  
 122 its support, enabling it to generate trajectories that were previously impossible.

125 

##### 3.1.1 THEORETICAL CONTEXT: THE LIMITS OF STANDARD RL

127 To ground our proof, we first adopt the theoretical framework proposed by Wu et al. (2025), which  
 128 formalizes the limitations of standard on-policy reinforcement learning (DeepSeek, 2025; Lambert  
 129 et al., 2024; Schulman et al., 2017) on training LLMs. We briefly introduce the key concepts (a  
 130 detailed review is provided in Appendix B).

131 The **support** of a model with distribution  $p$ ,  $\text{supp}(p)$ , is the set of all trajectories it can generate  
 132 with non-zero probability. The central limitation of RLVR, as established by Wu et al. (2025), is the  
 133 **Support Preservation Theorem**. It states that the support of the RL-trained policy is a subset of  
 134 the support of the base model. The Support Preservation Theorem formalizes the “invisible leash”:  
 135 RLVR can only re-weight probabilities within the model’s pre-existing support, but cannot expand it.

136 A more practical variant of support  $\text{supp}(p)$  is the **empirical support**,  $\text{supp}_\varepsilon(p)$ , which only includes  
 137 trajectories with a probability greater than a small threshold  $\varepsilon$ ; in what follows, all statements will be  
 138 made under this empirical-support view, within which we establish a strictly stronger and practical  
 139 result on TIR models.

141 

##### 3.1.2 PROOF OF SUPPORT EXPANSION

143 We consider two types of LLMs in this work. A pure-text model is a standard language model with  
 144 distribution  $q_{\text{text}}$ . We compare this to a TIR model with distribution  $p_{\text{TIR}}$ , which pairs a language  
 145 model with a deterministic external oracle (e.g., a Python interpreter). **Our goal here is to study the**  
 146 **reachable trajectory space induced by the external tool, not the outcome of RL training on tool use.**  
 147 **Therefore, throughout this section we assume that the pure-text model  $q_{\text{text}}$  and the TIR model  $p_{\text{TIR}}$**   
 148 **share exactly the same underlying language model parameters. The only difference is that the TIR**  
 149 **model is equipped with additional deterministic transitions provided by the tool.** Now we present the  
 150 main theorem and its proof sketch (a complete proof is provided in Appendix C):

151 **Theorem 3.1** (Strict Expansion of Empirical Support via Tool Integration). *There exists an  $\varepsilon > 0$*   
 152 *and a family of problem instances such that the empirical support of a pure-text model is a strict*  
 153 *subset of the empirical support of a tool-integrated model:*

$$154 \quad \text{supp}_\varepsilon(q_{\text{text}}) \subset \text{supp}_\varepsilon(p_{\text{TIR}}).$$

157 *Proof Sketch.* **(Inclusion  $\subseteq$ )** is straightforward. **Because, given that both models share the same**  
 158 **underlying language-model parameters, the TIR model can reproduce any natural-language trajectory**  
 159 **generated by the pure-text model with exactly the same probability. Thus every pure-text trajectory**  
 160 **remains reachable in the TIR environment with unchanged probability.** **(Strictness  $\subset$ )** relies on a  
 161 constructive proof using a standard cryptographic primitive: *random oracle*. The tool-integrated  
 model can deterministically solve the oracle problem in a single step. In contrast, the pure-text

162 model must guess the high-entropy  $m$ -bit output, succeeding with a probability  $(2^{-m})$  that becomes  
 163 negligible for any practical threshold  $\varepsilon$ . Thus, a correct trajectory exists that is within the empirical  
 164 support of  $p_{\text{TIR}}$  but not of  $q_{\text{text}}$ .  $\square$   
 165

166 The use of a random oracle here is purely idealized and serves as an existence proof: it witnesses  
 167 that there exist deterministic external tools for which no pure-text next-token model can assign  
 168 non-negligible probability to the correct trajectory. We further show in Appendix C how the same  
 169 argument extends to realistic tools.

170 We have shown that  $\text{supp}(q_{\text{text}})$  is a strict subset of  $\text{supp}(p_{\text{TIR}})$ . Unlike pure-text models, which  
 171 are constrained by Support Preservation Theorem, tool integration breaks the “invisible leash” by  
 172 introducing new, deterministic state transitions, thereby creating a strict expansion of the model’s  
 173 support.

### 175 3.2 TOKEN EFFICIENCY AND FEASIBLE SUPPORT UNDER A BUDGET

177 The proof in the previous section establishes that a tool-integrated model can generate trajectories that  
 178 are impossible for a pure-text model. This, however, raises a deeper question: can a pure-text model  
 179 achieve the same outcomes by *simulating* the computational process through natural language? While  
 180 the resulting trajectories  $y$  may differ syntactically ( $y_{\text{text}} \neq y_{\text{TIR}}$ ), they might represent the *same*  
 181 underlying problem-solving strategy. To properly evaluate this, we must move beyond comparing  
 182 trajectories based on string identity and instead assess them on their semantic content and efficiency.  
 183 This motivates our analysis of *token efficiency*.

#### 184 3.2.1 THE CONCEPT OF TOKEN EFFICIENCY

186 A key distinction between programmatic and natural language solutions is their *token efficiency*: the  
 187 compactness with which a solution is represented. For any task involving iteration or recursion, a  
 188 programmatic representation offers a scalable, abstract description with a near-constant token cost,  
 189 e.g.,  $O(1)$ . In contrast, a natural language trace that simulates the same process must enumerate  
 190 each computational step, leading to a token cost that scales with the size of the computation. The  
 191 tables in Appendix F illustrate this stark disparity for common algorithmic patterns: simple iteration  
 192 (Table 1), large linear systems (Table 2), dynamic programming (Table 3), and graph search (Table  
 193 4). In each case, the programmatic solution remains a concise, scalable representation, while the  
 194 natural language simulation becomes a verbose, concrete enumeration that is untenable for non-trivial  
 195 problem sizes.

#### 196 3.2.2 FEASIBLE SUPPORT UNDER A TOKEN BUDGET

198 The fundamental disparity in token efficiency motivates a more *practical, budget-aware* analysis of a  
 199 model’s capabilities, moving beyond theoretical possibilities to what is achievable within operational  
 200 constraints. To formalize this, we first define the total *token cost* of a trajectory,  $\text{cost}(y)$ , as the sum  
 201 of all tokens consumed (i.e., prompt, model generation, and tools I/O), which must not exceed the  
 202 model’s context budget  $B$ . This allows us to define the set of strategies a model can feasibly execute:

203 **Definition 3.2** (Computational Equivalence Class). Two trajectories,  $y_1$  and  $y_2$ , are computationally  
 204 equivalent, denoted  $y_1 \sim y_2$ , if they solve the same problem  $x$  by implementing the same core  
 205 algorithm. This relation partitions the space of all trajectories  $\mathcal{Y}$  into equivalence classes, where each  
 206 class  $[y]$  represents a distinct algorithmic “idea” or “strategy”.

207 **Definition 3.3** (Feasible Support under Budget  $B$ ). An algorithmic strategy, represented by equi-  
 208 valence class  $[y]$ , is within the feasible support of a model  $M$  under token budget  $B$ , denoted  
 209  $[y] \in \text{supp}_B(M)$ , if and only if there exists at least one trajectory  $y' \in [y]$  such that  $M(y'|x) > 0$   
 210 and its token cost( $y'$ ) does not exceed the budget:

$$211 \exists y' \in [y] \text{ s.t. } M(y'|x) > 0 \text{ and } \text{cost}(y') \leq B.$$

213 This definition captures a model’s practical ability to realize a problem-solving strategy within  
 214 operational constraints. With this formal framework in place, we can now state our central claim  
 215 regarding the practical supremacy of tool-integrated models and its proof sketch (a detailed proof is  
 provided in Appendix D):

216

**Theorem 3.4** (Strict Supremacy of Tool-Integrated Feasible Support). *For any non-trivial algorithmic problem class and any token budget  $B$ , there exists a problem size  $n_B$  such that the feasible support of a pure-text model is a strict subset of the feasible support of a tool-integrated model:*

$$\text{supp}_B(q_{\text{text}}) \subset \text{supp}_B(p_{\text{TIR}}).$$

221

222

*Proof Sketch.* **(Inclusion  $\subseteq$ )** holds because a tool-integrated model can always operate within the pure-text paradigm. **(Strictness  $\subset$ )** follows directly from the divergent scaling properties of the natural language. For any finite budget  $B$ , we can choose a problem size  $n_B$  large enough that the token cost of a natural language simulation exceeds  $B$ , while the  $O(1)$  programmatic representation remains well within budget. Thus, the algorithmic strategy is feasible for  $p_{\text{TIR}}$  but not for  $q_{\text{text}}$ .  $\square$

227

228

The theorem crystallizes the practical implications of token efficiency. It establishes that for any finite computational budget, there is a vast class of algorithmic strategies that pure-text models are fundamentally incapable of executing. Not because the solution is unknowable, but because its expression in natural language is too *verbose*. Tool integration is therefore not merely a convenience; it is a necessity for expanding the set of algorithmic approaches that LLMs can feasibly deploy. This provides a strong argument for a paradigm where LLMs act as reasoning engines that delegate complex computational tasks to specialized, efficient tools.

234

235

The analysis above focuses on token efficiency because the context window is the primary hard constraint for LLMs: a strategy is only usable if it can be represented within the available tokens, regardless of its external computation time. Although external tools do incur computational cost, in practical systems they are introduced exactly because they execute specific tasks much more efficiently than simulating the same process through natural-language traces. It ensures that TIR remains more efficient when accounting for the computational cost of the tool. As a result, incorporating tool cost does not change the underlying conclusion of this section.

241

242

### 3.3 ALGORITHMIC IMPROVEMENT: ADVANTAGE SHAPING FOR EARLY CODE INVOCATION

243

244

The TIR models often default to a conservative strategy: completing the majority of their abstract reasoning via text before invoking the code interpreter for the final-step calculation or verification. This overlooks a potentially more powerful paradigm where the interpreter is used as an exploratory tool throughout the reasoning process. We hypothesize that encouraging the model to invoke code *earlier* could foster a more dynamic, flexible, and hypothesis-driven reasoning style, potentially unlocking novel problem-solving strategies.

250

251

To encourage earlier tool use, we first tried adding an early-code bonus to the reward function, but this approach proved highly unstable. In GRPO-like algorithms, group normalization cancels the primary correctness signal when all samples in a group are correct, catastrophically amplifying the auxiliary bonus and distorts the learning objective (see Appendix G for a detailed analysis).

254

255

To circumvent the distorting effects of reward normalization, we developed a more robust method that we term Advantage Shaping Policy Optimization (**ASPO**). Instead of manipulating the reward, we directly modify the final advantage value after the standard correctness-based advantage  $A_{\text{correct}}$  has been calculated. For any response  $i$  that is both correct and contains code, we compute the new advantage  $A_i$  as follows:

259

260

261

$$A_i = A_{\text{correct},i} + \text{clip}\left(\delta \cdot \frac{p_i - \text{mean}(\mathbf{p})}{\text{mean}(\mathbf{L})}, -k \cdot A_{\text{correct},i}, k \cdot A_{\text{correct},i}\right),$$

262

263

264

265

266

267

where  $\mathbf{p}$  and  $\mathbf{L}$  are the sets of first code invocation positions and total response lengths for all correct, code-containing responses within the group. Furthermore,  $\delta$  is a negative coefficient to encourage early code invocation, and  $k$  is a clipping hyperparameter that bounds the magnitude of auxiliary advantage within a proportion of the basic advantage of correctness. **Importantly, the auxiliary term is applied only to trajectories that are both correct and contain tool call; trajectories with incorrect final answers never receive any bonus, regardless of their tool-use behavior.**

268

269

This formulation has several key merits, primarily by circumventing the uncontrollable effects of advantage normalization inherent to reward-based modifications. First, it addresses a critical flaw in the reward-based approach: the inability to guarantee a positive advantage for all correct answers.

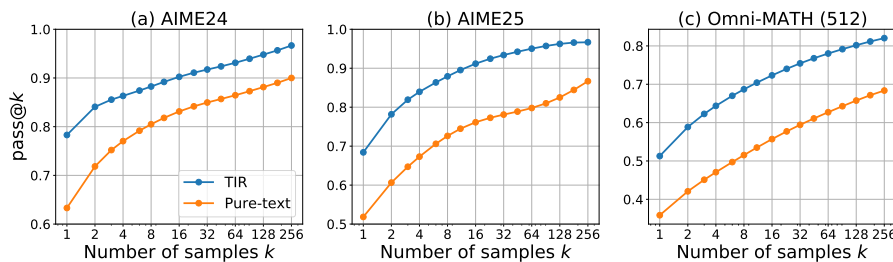
270 After adding the auxiliary reward, a correct response’s total reward could fall below the group average,  
 271 leading to a negative GRPO normalized advantage, which effectively punishes a correct solution.  
 272 Second, the GRPO normalization process introduces uncontrollable volatility: the  $\text{std}(\mathbf{R})$  in the  
 273 denominator unpredictably scales the auxiliary signal, making its influence inconsistent across groups.  
 274

275 Our ASPO algorithm resolves both issues. By applying a clipped bias directly to  $A_{\text{correct}}$ , we ensure  
 276 the final advantage remains positive and that the early-code incentive is always a subordinate nudge,  
 277 never overwhelming the primary objective of correctness. Furthermore, this approach bypasses the  
 278 volatile scaling effect of  $\text{std}(\mathbf{R})$  entirely. Besides, the auxiliary advantage involves  $p - \text{mean}(p)$ . As a  
 279 result, within the correct-and-tool subgroup, ASPO essentially performs a zero-sum redistribution of  
 280 advantage (ignoring clipping effects). It does not artificially inflate the total advantage mass for this  
 281 subgroup. The total advantage mass of “tool-use” or “correct-answer” also remains unchanged. From  
 282 this perspective, it does not directly encourage more tool calls. Rather, it re-ranks the responses in the  
 283 correct-and-tool subgroup, expressing a preference for early invocation over late invocation among  
 284 the correct-and-tool responses. Finally, the choice to normalize the code invocation position by the  
 285 mean response length  $\text{mean}(\mathbf{L})$  rather than the standard deviation of positions  $\text{std}(\mathbf{p})$  is deliberate.  
 286 The latter is unstable: when invocation positions in a group are tightly clustered, a small  $\text{std}(\mathbf{p})$  would  
 287 excessively amplify the signal, whereas a more stable denominator like  $\text{mean}(\mathbf{L})$  is consistent and  
 288 meaningful. This method allows us to stably and effectively encourage early code invocation, the  
 289 empirical results of which are detailed in Section 4.4.  
 290

291 In essence, ASPO provides a general and robust framework for guiding a model’s behavior towards  
 292 desired styles or properties without compromising the primary learning objective (e.g., accuracy). By  
 293 directly manipulating the advantage values, ASPO avoids the instabilities that can arise from altering  
 294 the reward function, particularly in GRPO-like algorithms that rely on reward normalization. This  
 295 method ensures that the incentive for the desired behavior (in this case, earlier code invocation) acts  
 296 as a stable adjustment. The core principles of ASPO could be *readily adapted* to encourage other  
 297 desirable behaviors in a variety of scenarios, offering a reliable approach to shape model conduct  
 298 while preserving training stability and overall task performance.  
 299

## 4 EXPERIMENTS

300 All experiments are based on the Qwen3-8B model (Qwen, 2025). We compare our proposed Tool-  
 301 Integrated Reasoning (TIR) model against a pure-text RL baseline (see Figure 5 in Appendix H). For  
 302 training, we used a 10,000-problem subset of the DAPO dataset (Yu et al., 2025), which is sufficient  
 303 for our goal of understanding TIR mechanisms rather than achieving state-of-the-art benchmark scores.  
 304 Both models were trained using the DAPO algorithm (Yu et al., 2025), a variant of GRPO (DeepSeek,  
 305 2025). Our primary evaluation benchmarks are AIME24, AIME25, and Omni-MATH-512, a curated  
 306 set of 512 challenging problems from the Omni-MATH dataset (Gao et al., 2024). A detailed  
 307 experimental setup is provided in Appendix H.  
 308



316 Figure 1: Pass@ $k$  curves for the TIR (RL trained) and pure-text models (Qwen3-8B) across three  
 317 benchmarks: (a) AIME24, (b) AIME25, and (c) Omni-MATH-512. The pure-text model here  
 318 corresponds to the vanilla Qwen3-8B base model without RL fine-tuning. This choice is intentional  
 319 and conservative: prior work (Yue et al., 2025) reports that RL often decreases pass@ $k$  performance  
 320 at large  $k$ . We also evaluated the AIME25 pass@ $k$  for RL-trained pure-text model, finding that the  
 321 vanilla Qwen3-8B model performs better than its RL counterpart at large  $k$ . We therefore adopt the  
 322 stronger vanilla baseline to better characterize the capability ceiling. The detailed numerical data  
 323 corresponding to this figure are provided in the Appendix I.  
 324

324  
325

## 4.1 PASS@K EXPERIMENTS: TIR BREAKS THE CAPABILITY CEILING

326  
327  
328  
329

To empirically test our theoretical claims, this section investigates whether TIR can overcome the capability ceiling observed in pure-text models (Yue et al., 2025; Wu et al., 2025). Similar to Yue et al. (2025) and others, we use the pass@ $k$  metric, with low-variance estimation from Chen et al. (2021), as it provides a robust measure of a model’s underlying problem-solving potential.

330  
331  
332  
333  
334  
335  
336  
337  
338  
339  
340  
341  
342  
343  
344  
345  
346  
347  
348

Figure 1 presents the macroscopic evidence from our experiments. It plots the pass@ $k$  curves for both the TIR model (RL trained) and the pure-text baseline (Qwen3-8B) across our three evaluation benchmarks, with the max  $k$  of 256. The results are unequivocal: on AIME24, AIME25, and Omni-MATH-512, the TIR model’s performance curve is consistently and significantly higher than that of the pure-text model. Crucially, we observe *no intersection* between the curves, even as  $k$  increases to 256. This stands in stark contrast to previous findings where RL-trained text models, while improving pass@1, often do so at the cost of the broader capability envelope, eventually being surpassed by the base model at high values of  $k$  (Yue et al., 2025). Our results show TIR does not suffer from this trade-off; it elevates the *entire* pass@ $k$  curve. **We also show that this phenomenon is stable under different temperature in Appendix J**

349  
350  
351  
352  
353  
354  
355  
356  
357  
358  
359  
360  
361  
362  
363  
364

To further understand this performance gain at a per-problem level, we visualize the “flow of solvability” on the Omni-MATH-512 dataset in Figure 2. This Sankey diagram illustrates how the solvability status of individual problems changes when moving from the pure-text model to the TIR model (samples  $k = 256$  responses per problem). We categorize the problems into four distinct groups as Wu et al. (2025): **Capability Expansion**: Problems the pure-text model fails to solve but the TIR model succeeds on; **Capability Preservation**: Problems solved by both models; **Capability Shrinkage**: Problems solved by the pure-text model but not by the TIR model; **Jointly Unsolved**: Problems that neither model can solve. The diagram reveals a massive net gain in problem-solving capability. The Capability Expansion set contains 15.4% problems, whereas the Capability Shrinkage set contains only 1.8% (**In Appendix L we show that this small shrinkage is due to sampling variance and RL training**). This provides direct empirical validation for our theoretical argument in Section 3, demonstrating that TIR facilitates a practically significant expansion of the model’s effective support.

365  
366  
367  
368  
369  
370  
371  
372  
373  
374

In summary, both macroscopic pass@ $k$  analysis and microscopic problem-level tracking confirm that tool-integrated reasoning decisively breaks the capability ceiling of its pure-text counterpart, enabling the model to solve a wide range of problems that were previously out of its reach.

## 4.2 BENEFITS OF TIR EXTEND BEYOND COMPUTATIONALLY-INTENSIVE PROBLEMS

375  
376  
377

A crucial question arises from our initial findings: is the observed capability expansion of TIR merely an *artifact* of solving problems that are inherently algorithmic? The most direct yet naive interpretation of TIR’s success is that it simply offloads complex arithmetic, acting as a superior *calculator*. However, a more nuanced counterargument posits that TIR’s effectiveness, while beyond simple calculation, is still confined to problems whose structure can be directly mapped to a known algorithm such as exhaustive search in combinatorics. This perspective suggests that TIR improves the model’s capability on problems that are computationally-intensive or inherently algorithmic, but offers *little advantage* when the problem is highly abstract.

To rigorously test our hypothesis, we first introduce the concept of “algorithmic friendliness”, which is defined as a measure of how reliant a problem’s solution is on standard computation *versus* deep mathematical insight. To operationalize this concept, we developed a detailed five-point rubric for classifying problems, as presented in Appendix M. This scale ranges from a score of 1 for problems

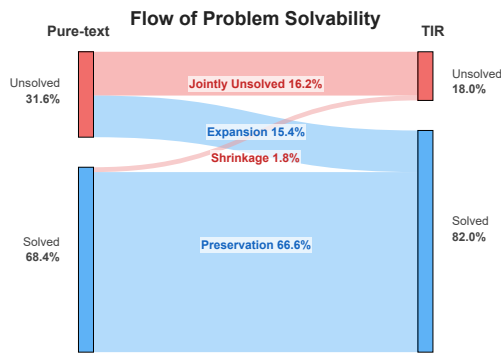


Figure 2: The flow of problem solvability on Omni-MATH-512 when transitioning from the pure-text model to the TIR model, evaluated at  $k = 256$ . A detailed version is provided in Appendix K.

378 that are fundamentally abstract and non-computational, to 5 for those solvable by a direct application  
 379 of a textbook algorithm. We then applied this rubric to classify each problem in the Omni-MATH-512  
 380 dataset. This classification was performed by providing both the problem statement and its solution  
 381 idea to the Gemini 2.5 Pro API (Gemini, 2025), which then assigned a score based on the rubric.  
 382 The resulting distribution of problem types, shown in Figure 8(f) (Appendix N), reveals a crucial  
 383 characteristic of the dataset. Contrary to being biased towards highly algorithmic problems, the  
 384 distribution’s peak is concentrated in the medium friendliness categories (scores 2, 3 and 4). This  
 385 confirms that Omni-MATH-512 serves as a fair and challenging testbed for our analysis, not one  
 386 skewed towards problems with simple computational solutions. **To check this classification, we**  
 387 **manually inspected all problems in the lowest-friendliness bucket** (24 items with scores between  
 388 1.0 and 1.5) and found them consistent with the rubric. We also queried Gemini multiple times per  
 389 problem and averaged the scores to reduce stochastic variation. Since the friendliness labels are only  
 390 used for grouping, rather than as supervision or evaluation signals, this level of validation is sufficient  
 391 for our analysis.

392 Figure 8(a)-(e) (Appendix N) presents our *core findings*. It displays the pass@ $k$  curves for the TIR  
 393 and pure-text models, grouped by the algo friendliness of the problems. As expected, the performance  
 394 gap between the two models is most pronounced for problems with high friendliness (scores 4.0-5.0),  
 395 where TIR’s ability to execute algorithms directly provides a massive advantage (Figure 8(d),(e)). The  
 396 *most critical* finding, however, comes from the lowest friendliness group (scores 1.0-2.5). Even for  
 397 these problems, which depend heavily on abstract reasoning and are ill-suited to direct computation,  
 398 the TIR model maintains a significant and consistent performance advantage over the pure-text  
 399 baseline, outperforming it by approximately 9% in pass@256 accuracy (Figure 8(a),(b)).

400 This result demonstrates that the benefits of TIR are not confined to easily programmable problems.  
 401 The tool serves a more profound purpose than acting as a simple calculator or a direct algorithm-  
 402 implementer. It suggests that the model is leveraging the code interpreter in more complex and  
 403 sophisticated ways, which we will investigate in the next subsection.

#### 4.3 EMERGENT COGNITIVE PATTERNS OF TOOL INTEGRATION

404 To understand *how* TIR is effective beyond purely algorithmic problems, our qualitative analysis  
 405 identified three recurring patterns of code utilization. These patterns reveal a sophisticated interplay  
 406 where the model is not just *using* a tool, but fundamentally *thinking with* it. **Pattern 1: Insight-  
 407 to-computation transformation.** The model first engages in text-based reasoning to transform an  
 408 abstract problem into a computationally tractable form. It then invokes the interpreter to execute a  
 409 genuine algorithm (e.g., search, enumeration, DP) on this newly formulated sub-problem. **Pattern  
 410 2: Exploration and verification via code.** For problems with unclear solution paths, the model  
 411 uses the interpreter as an interactive sandbox. It formulates conjectures, writes short code snippets to  
 412 test them, and iteratively refines its strategy based on the feedback, allowing it to discover insights  
 413 through empirical experimentation. **Pattern 3: Offloading complex calculation.** In the most direct  
 414 usage, the model delegates complex or tedious calculations to the interpreter. This minimizes the  
 415 risk of unforced computational errors that could derail a correct line of reasoning. The first two  
 416 patterns represent a fundamental departure from pure-text reasoning, constituting new *Computational*  
 417 *Equivalence Classes* that are infeasible for pure-text models due to prohibitive token costs (i.e., they  
 418 lie outside the *Feasible Support under Budget B*). Such dynamic and flexible code invocation enables  
 419 the TIR model to break the capability ceiling of its pure-text counterpart. Detailed analysis and  
 420 examples of these patterns are provided in Appendix O.

#### 4.4 EMPIRICAL ANALYSIS OF ASPO FOR EARLY CODE INVOCATION

421 In this section, we empirically validate our ASPO algorithm, designed to encourage earlier code  
 422 invocation. We aim to answer two primary questions: (1) Does this method maintain training stability  
 423 and final task performance, unlike the naive reward-based approach? (2) Does it effectively and  
 424 controllably alter the model’s tool-use behavior as intended? We test our baseline model against the  
 425 unstable reward-based approach and two variants of our ASPO algorithm: a *conservative* setting  
 426 ( $\delta = -2.0, k = 0.7$ ) and an *aggressive* setting ( $\delta = -2.5, k = 0.9$ ).

427 **Stability and performance remain uncompromised.** Figure 3 provides a clear validation of our  
 428 method’s stability. As mentioned in our analysis in Section 3, the naive reward-based approach

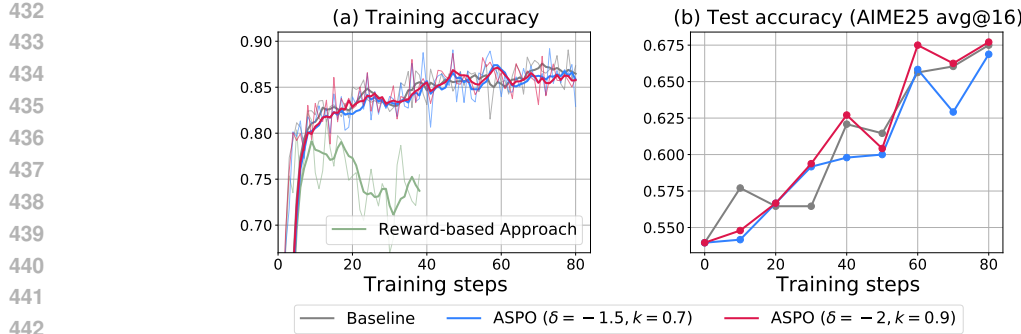


Figure 3: The (a) training and (b) testing accuracy of the baseline (the standard DAPO algorithm (Yu et al., 2025) with only final-answer reward) and ASPO algorithm.

quickly becomes unstable, causing the training reward to collapse (Figure 3(a)). In stark contrast, the training curves for our ASPO algorithm with both conservative and aggressive settings remain stable and almost perfectly aligned with the baseline. Furthermore, this stability does not come at the cost of final performance. Figure 3(b) shows that the final “avg@16” accuracy on AIME25 for both variants is statistically indistinguishable from the baseline. This is a crucial result: our method successfully avoids the pitfalls of reward modification, ensuring that the primary goal of solving the problem correctly is not sacrificed.

**A significant shift in cognitive behavior.** Having established the method’s safety, we now demonstrate its effectiveness in reshaping the model’s reasoning strategy. Figure 4 presents a comprehensive analysis of the model’s code-use behavior on AIME25, averaged over 16 responses per question. The results show a dramatic and targeted shift. The most significant change is in the code invocation timing (Figure 4(b)), where the average position of the first code call is brought forward from 4,000 tokens in the baseline down to 1,000 tokens. Concurrently, the model becomes a much more active tool user: the average number of code rounds per problem more than doubles, from 1.3 to 3.3 (Figure 4(e)), and the code ratio approaches nearly 100%, indicating that using the interpreter becomes a default part of the model’s process (Figure 4(c)). This behavioral shift is starkly evident when examining the distribution of responses for a single challenging problem. For instance, on Q30 of the AIME25, the baseline model exhibited reluctant and inconsistent tool use: out of 16 independent responses, four failed to make a single code call, and the median number of invocations was just 2. In stark contrast, our ASPO-trained model integrated the tool as an indispensable part of its problem-solving process. It invoked the code in all 16 responses for the same problem, and the median number of tool calls increased from 2 to 13. More significantly, a quarter of the responses demonstrated highly iterative behavior, making more than 20 tool calls, which is entirely absent in the GRPO-trained baseline. This shows a clear transformation from a conservative, late-stage “calculator” usage pattern to an early, iterative, and exploratory “interactive partner” paradigm.

**Controllability and absence of reward hacking.** Importantly, this behavioral shift is achieved without inducing reward hacking. We manually inspected a large number of samples and found no instances of the model inserting trivial or meaningless code early in its response merely to satisfy the incentive. The stability of the final task accuracy (Figure 3(b)) and the code pass ratio (Figure 4(d)) further substantiates this. Finally, the difference between the conservative and aggressive settings demonstrates that the degree of behavioral change is tunable via the hyperparameters  $\delta$  and  $k$ .

## 5 CONCLUSIONS

In this work, we presented a comprehensive investigation into the foundational mechanisms of Tool-Integrated Reasoning (TIR). We moved beyond empirical demonstrations to establish a formal theoretical framework explaining its effectiveness. Our core theoretical contribution is the proof that TIR enables a strict expansion of both the empirical and feasible support of an LLM, breaking the “invisible leash” that constrains pure-text models and making complex algorithmic strategies practically achievable within finite token budgets. On the algorithmic front, we identified the instability of reward shaping for guiding model behavior in TIR systems and proposed Advantage

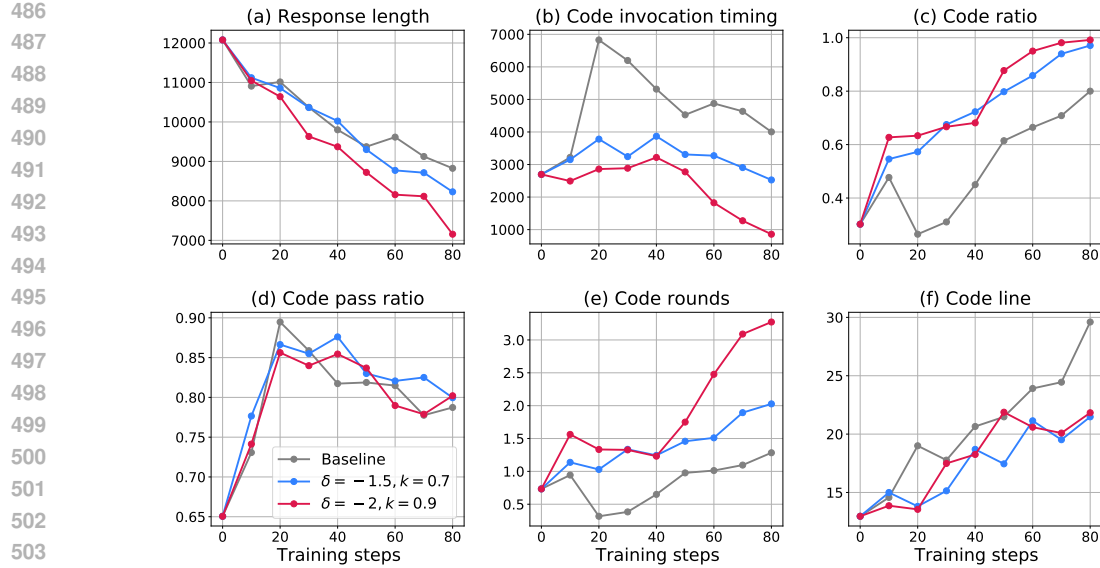


Figure 4: Evaluation results of the baseline and ASPO algorithm on AIME25. (a) Response length, (b) code invocation timing, (c) code ratio, (d) code pass ratio, (e) code rounds and (f) code lines.

Shaping Policy Optimization (ASPO), a stable and effective alternative that directly modifies the advantage function.

Our experiments provided strong empirical validation for these claims. We demonstrated that TIR model equipped with a Python interpreter decisively surpasses the performance of pure-text models across challenging mathematical reasoning benchmarks. Our analysis, using a novel “algorithmic friendliness” metric, revealed that TIR’s benefits are universal, extending even to problems that are highly abstract and less amenable to direct computation. Qualitative analysis further uncovered the sophisticated, emergent cognitive patterns that arise from the synergy between LLM reasoning and tool execution.

Ultimately, our findings advocate for a paradigm shift: viewing LLMs not as monolithic problem-solvers, but as core reasoning engines that intelligently delegate computational tasks to specialized, efficient tools. The principles and methods developed here, particularly ASPO, open avenues for more nuanced and stable control over the behavior of powerful tool-integrated agents.

## REFERENCES

Fei Bai, Yingqian Min, Beichen Zhang, Zhipeng Chen, Wayne Xin Zhao, Lei Fang, Zheng Liu, Zhongyuan Wang, and Ji-Rong Wen. Towards effective code-integrated reasoning. *arXiv preprint arXiv:2505.24480*, 2025.

Mark Chen, Jerry Tworek, Heewoo Jun, Qiming Yuan, Henrique Ponde De Oliveira Pinto, Jared Kaplan, Harri Edwards, Yuri Burda, Nicholas Joseph, Greg Brockman, et al. Evaluating large language models trained on code. *arXiv preprint arXiv:2107.03374*, 2021.

Team DeepSeek. DeepSeek-R1 incentivizes reasoning in LLMs through reinforcement learning. *Nature*, 645:633–638, 2025.

Jiazhan Feng, Shijue Huang, Xingwei Qu, Ge Zhang, Yujia Qin, Baoquan Zhong, Chengquan Jiang, Jinxin Chi, and Wanjun Zhong. ReTool: Reinforcement learning for strategic tool use in LLMs. *arXiv preprint arXiv:2504.11536*, 2025.

Bofei Gao, Feifan Song, Zhe Yang, Zefan Cai, Yibo Miao, Qingxiu Dong, Lei Li, Chenghao Ma, Liang Chen, Runxin Xu, et al. Omni-math: A universal olympiad level mathematic benchmark for large language models. *arXiv preprint arXiv:2410.07985*, 2024.

540 Team Gemini. Gemini 2.5: Pushing the frontier with advanced reasoning, multimodality, long context,  
 541 and next generation agentic capabilities. *arXiv preprint arXiv:2507.06261*, 2025.  
 542

543 Bowen Jin, Hansi Zeng, Zhenrui Yue, Jinsung Yoon, Sercan Arik, Dong Wang, Hamed Zamani, and  
 544 Jiawei Han. Search-R1: Training LLMs to reason and leverage search engines with reinforcement  
 545 learning. *arXiv preprint arXiv:2503.09516*, 2025.

546 Nathan Lambert, Jacob Morrison, Valentina Pyatkin, Shengyi Huang, Hamish Ivison, Faeze Brahman,  
 547 Lester James V Miranda, Alisa Liu, Nouha Dziri, Shane Lyu, et al. Tülu 3: Pushing frontiers in  
 548 open language model post-training. *arXiv preprint arXiv:2411.15124*, 2024.  
 549

550 Kuan Li, Zhongwang Zhang, Huirong Yin, Liwen Zhang, Litu Ou, Jialong Wu, Wenbiao Yin, Baixuan  
 551 Li, Zhengwei Tao, Xinyu Wang, et al. WebSailor: Navigating super-human reasoning for web  
 552 agent. *arXiv preprint arXiv:2507.02592*, 2025a.

553 Xuefeng Li, Haoyang Zou, and Pengfei Liu. ToRL: Scaling tool-integrated RL. *arXiv preprint  
 554 arXiv:2503.23383*, 2025b.  
 555

556 OpenAI. Introducing GPT-5. Blog post, Aug 2025a. URL <https://openai.com/index/gpt-5/>. Accessed on August 22, 2025.  
 557

558 OpenAI. Introducing o3 and o4-mini. Blog post, April 2025b. URL <https://openai.com/index/introducing-o3-and-o4-mini/>. Accessed on August 22, 2025.  
 559

560 Team Qwen. Qwen3 technical report. *arXiv preprint arXiv:2505.09388*, 2025.  
 561

562 John Schulman, Filip Wolski, Prafulla Dhariwal, Alec Radford, and Oleg Klimov. Proximal policy  
 563 optimization algorithms. *arXiv preprint arXiv:1707.06347*, 2017.  
 564

565 Zhihong Shao, Peiyi Wang, Qihao Zhu, Runxin Xu, Junxiao Song, Xiao Bi, Haowei Zhang,  
 566 Mingchuan Zhang, YK Li, Yang Wu, et al. DeepSeekMath: Pushing the limits of mathematical  
 567 reasoning in open language models. *arXiv preprint arXiv:2402.03300*, 2024.  
 568

569 Richard S Sutton, Andrew G Barto, et al. *Reinforcement learning: An introduction*, volume 1. MIT  
 570 press Cambridge, 1998.  
 571

572 Fang Wu, Weihao Xuan, Ximing Lu, Zaid Harchaoui, and Yejin Choi. The invisible leash: Why  
 573 RLVR may not escape its origin. *arXiv preprint arXiv:2507.14843*, 2025.  
 574

575 xAI. Grok 4. Blog post, Jul 2025. URL <https://x.ai/blog/grok-4>. Accessed on August  
 22, 2025.  
 576

577 Zhongwen Xu, Xianliang Wang, Siyi Li, Tao Yu, Liang Wang, Qiang Fu, and Wei Yang. Agents play  
 578 thousands of 3D video games. *arXiv preprint arXiv:2503.13356*, 2025.  
 579

580 Zhenghai Xue, Longtao Zheng, Qian Liu, Yingru Li, Zejun Ma, and Bo An. SimpleTIR: End-to-end  
 581 reinforcement learning for multi-turn tool-integrated reasoning. *arXiv preprint arXiv:2509.02479*,  
 582 2025.  
 583

584 Qiyi Yu, Zheng Zhang, Ruofei Zhu, Yufeng Yuan, et al. DAPO: An open-source LLM reinforce-  
 585 ment learning system at scale. *arXiv preprint arXiv:2503.14476*, 2025.  
 586

587 Yang Yue, Zhiqi Chen, Rui Lu, Andrew Zhao, Zhaokai Wang, Shiji Song, and Gao Huang. Does  
 588 reinforcement learning really incentivize reasoning capacity in LLMs beyond the base model?  
 589 *arXiv preprint arXiv:2504.13837*, 2025.  
 590

## A LLM USAGE

591 During the preparation of this work, we used LLM to aid in polishing the manuscript and improving  
 592 language. All final content was reviewed and revised by the authors to ensure its accuracy and  
 593 originality. The core ideas, methods, and conclusions of the paper are solely the work of the authors.

594 **B THE THEORETICAL BACKGROUND**

595

596 To ground our proof, we adopt the theoretical framework proposed by Wu et al. (2025), which  
 597 formalizes the limitations of standard on-policy reinforcement learning (DeepSeek, 2025; Lambert  
 598 et al., 2024; Schulman et al., 2017) on training LLMs.

599 **Definition B.1** (Support of a Model (adapted from (Wu et al., 2025))). Let  $\mathcal{Y}$  be the space of all  
 600 possible generative trajectories. The support of a model with distribution  $p(y|x)$  is the set of all  
 601 trajectories that can be generated with a non-zero probability for a given prompt  $x$ :

$$602 \text{supp}(p) := \{y \in \mathcal{Y} \mid p(y|x) > 0\}$$

603

604 **Definition B.2** (Empirical Support (from Wu et al. (2025))). For a threshold  $\varepsilon > 0$ , define the  
 605 empirical support of  $p$  as

$$606 \text{supp}_\varepsilon(p) := \{y \in \mathcal{Y} \mid p(y|x) \geq \varepsilon\}.$$

607

608 This definition is central to understanding a model’s intrinsic capabilities. The following theorem  
 609 from Wu et al. (2025) establishes a key constraint for models trained with Reinforcement Learning  
 610 from Verifiable Rewards (RLVR) (Lambert et al., 2024; DeepSeek, 2025):

611 **Theorem B.3** (Support Preservation under RLVR (from Wu et al. (2025))). *Let  $\pi_\theta(y|x)$  be an  
 612 RLVR-trained policy distribution initialized from a base model with distribution  $q(y|x)$ . For any  
 613 prompt  $x$ , the support of the trained policy is a subset of the support of the base model:*

$$614 \text{supp}(\pi_\theta) \subseteq \text{supp}(q)$$

615 *This implies that if  $q(y^*|x) = 0$  for a correct trajectory  $y^*$ , then RLVR can never discover  $y^*$ .*

616

617 Theorem B.3 formalizes the “invisible leash”: RLVR can only re-weight probabilities within the  
 618 model’s pre-existing support. We next show a strictly stronger, practical statement under an empirical-  
 619 support view.

620

621 **C THE DETAILED PROOF OF SUPPORT EXPANSION**

622

623 We consider two types of LLMs in this work. A pure-text model is a standard language model  
 624 with distribution  $q_{\text{text}}$  that generates tokens exclusively from its vocabulary  $\mathcal{V}$ . We compare this to a  
 625 tool-integrated model, a system  $(M, \mathcal{O})$  with distribution  $p_{\text{TIR}}$ , which pairs a language model  $M$  with  
 626 a deterministic external oracle  $\mathcal{O}$  (e.g., a Python interpreter). The generative process for this model  
 627 includes not only probabilistic token generation from  $\mathcal{V}$  but also deterministic tool-use transitions.  
 628 In such a transition, the model  $M$  emits a tool call  $y_{\text{call}}$ , the oracle executes it, and the resulting  
 629 output  $y_{\text{out}} = \mathcal{O}(y_{\text{call}})$  is deterministically returned as the next state. **Our goal here is to study the  
 630 reachable trajectory space induced by the external tool, not the outcome of RL training on tool use.**  
 631 Therefore, we assume that the pure-text model and the TIR model share exactly the same underlying  
 632 language model parameters. The only difference is that the TIR model is equipped with additional  
 633 deterministic transitions provided by the tool.

634

635 Now we present the detailed proof of Theorem 3.1.

636

637 *Proof.* The proof proceeds in two parts. First, we establish the subset relationship ( $\subseteq$ ), and second,  
 638 we prove the relationship is strict ( $\neq$ ) by demonstrating the existence of trajectories accessible only  
 639 to the tool-integrated model.

640 **Part 1: Proving  $\text{supp}(q_{\text{text}}) \subseteq \text{supp}(p_{\text{TIR}})$**

641

642 Let  $y$  be an arbitrary trajectory in the support of the pure-text model, such that  $q_{\text{text}}(y|x) > 0$ . The  
 643 trajectory  $y$  consists exclusively of tokens from the vocabulary  $\mathcal{V}$ . **Because, given that both models  
 644 share the same underlying language-model parameters, the TIR model can reproduce any natural-  
 645 language trajectory generated by the pure-text model with exactly the same probability. Thus every  
 646 pure-text trajectory remains reachable in the TIR environment with unchanged probability.** Therefore,  
 647 for any  $y \in \text{supp}(q_{\text{text}})$ , it follows that  $y \in \text{supp}(p_{\text{TIR}})$ , establishing that  $\text{supp}(q_{\text{text}}) \subseteq \text{supp}(p_{\text{TIR}})$ .

648 **Part 2: Proving Strictness**

648 To prove strictness, we use a constructive approach based on a standard cryptographic primitive: a  
 649 *random oracle*. Let us consider a problem instance where the solution requires computing  $y_{\text{out}} =$   
 650  $H(x)$ , where  $H$  is a random oracle. A random oracle is a theoretical black box that, for any new  
 651 input query, returns an output chosen uniformly at random from its output space (e.g.,  $\{0, 1\}^m$ ), but  
 652 deterministically returns the same output for repeated queries of the same input. This construction is  
 653 theoretically convenient and serves as an idealization of practical cryptographic hash functions (e.g.,  
 654 SHA-256). For a model without access to the oracle, its only strategy to find  $y_{\text{out}}$  is to guess it. The  
 655 probability of correctly guessing a specific  $m$ -bit string is  $2^{-m}$ .

656 Now, consider a trajectory  $y^* = (y_{\text{prefix}}^*, y_{\text{out}}, y_{\text{suffix}}^*)$  that involves computing  $H(x)$ . We assume the  
 657 underlying language model for both  $p_{\text{TIR}}$  and  $q_{\text{text}}$  is identical. The tool-integrated model  $p_{\text{TIR}}$  can  
 658 invoke the oracle to obtain  $y_{\text{out}}$  deterministically. In contrast, the pure-text model,  $q_{\text{text}}$ , must guess  
 659  $y_{\text{out}}$  from an output space of size  $2^m$ , succeeding with a probability of only  $2^{-m}$ . Thus, the total  
 660 probabilities of producing  $y^*$  are directly related:

$$q_{\text{text}}(y^*|x) = p_{\text{TIR}}(y^*|x) \cdot 2^{-m}.$$

661 For any non-negligible probability  $p_{\text{TIR}}(y^*|x)$  and a sufficiently large  $m$ , the corresponding  $q_{\text{text}}(y^*|x)$   
 662 becomes arbitrarily small. We can therefore always choose an  $\varepsilon$  such that  $q_{\text{text}}(y^*|x) < \varepsilon \leq$   
 663  $p_{\text{TIR}}(y^*|x)$ . So we find that  $y^* \notin \text{supp}_\varepsilon(q_{\text{text}})$  while  $y^* \in \text{supp}_\varepsilon(p_{\text{TIR}})$ . This establishes strictness.  $\square$   
 664

### 666 On the Use of Random Oracle

667 The use of a random oracle in the strictness proof above is intentional and purely idealized. Its  
 668 purpose is existential: it demonstrates that there exist deterministic external transitions for which no  
 669 pure-text model can assign non-negligible probability to the correct trajectory, while a TIR model  
 670 retains a deterministic path.

671 While idealized, the random oracle proof can map directly to realistic scenarios and tools. We outline  
 672 two representative examples.

673 1. **Heavy numerical computation.** The core idea is that the probability of pure-text model generating  
 674 correct computation results decreases as computational tasks increase in complexity or length.  
 675 Consider a family of problems whose solution requires executing a sequence of  $N$  arithmetic or  
 676 numerical operations (e.g., iterative numerical solvers, time-stepping PDEs). Let a pure-text model  
 677 execute each primitive operation correctly with probability  $p < 1$ . Then the probability of emitting  
 678 a correct computational result decays exponentially. A TIR model, equipped with a deterministic  
 679 computational tool (e.g., numerical solver or Python interpreter), obtains the correct result via tool  
 680 call whose success probability does not depend on  $N$ .

681 2. **Knowledge Retrieval.** Querying an external database for unknown facts (e.g., specific weather  
 682 data) is mathematically equivalent to a Random Oracle. A pure-text model can only guess the correct  
 683 entry, with success probability decreasing as the answer length increases. In contrast, a TIR model  
 684 that issues a structured query to the database retrieves the correct entry deterministically.

685 These examples show that the random-oracle construction is not an unrealistic corner case, but a  
 686 convenient abstraction capturing a general principle: There exist practically relevant families of  
 687 problems whose solution probabilities for pure-text model vanish with problem size, while a TIR  
 688 model retains a deterministic solution trajectory. Thus, the strict support-expansion theorem captures  
 689 a structural phenomenon applicable well beyond idealized oracle settings.

## 692 D THE DETAILED PROOF OF FEASIBLE SUPPORT SUPREMACY

693 Here we present the detailed proof of Theorem 3.4.

694 *Proof.* The proof requires showing both inclusion ( $\subseteq$ ) and strictness ( $\neq$ ).

695 **Inclusion ( $\subseteq$ ):** Any algorithmic strategy that is feasibly executable by a pure-text model within  
 696 budget  $B$  is, by definition, also executable by a tool-integrated model that simply abstains from using  
 697 its tool.

698 **Strictness ( $\neq$ ):** We must show there exists an algorithmic class  $[y_A]$  in  $\text{supp}_B(p_{\text{TIR}})$  but not in  
 699  $\text{supp}_B(q_{\text{text}})$ . This follows directly from the divergent scaling properties of natural language versus

702 programmatic representations, as illustrated in Tables 1-4. For any algorithm whose pure-text  
 703 simulation cost scales with problem size  $n$  (e.g.,  $\Omega(n)$ ,  $\Omega(V + E)$ ), we can choose a size  $n_B$  such  
 704 that the cost exceeds any finite budget  $B$ . The programmatic representation, costing  $O(1)$ , remains  
 705 within budget. Thus, for a sufficiently large problem size, the corresponding algorithmic classes are  
 706 in the feasible support of  $p_{\text{TIR}}$  but not  $q_{\text{text}}$ , proving strict inclusion.  $\square$

## 708 E EXTENSIONS TO OTHER TOOLS AND INTERACTIONS WITH ENVIRONMENTS 709

710 Our arguments in Sections 3.1.2 and 3.2 extend beyond Python to a broad family of external tools  
 711 and interactive settings. At a high level, any interface that (i) affords *state transitions* not expressible  
 712 by next-token sampling alone and/or (ii) delivers *high information per token of I/O* will both expand  
 713 support (Section 3.1.2) and strictly enlarge feasible support under a token budget (Section 3.2).

714 **Search and Retrieval Agents.** Consider web search, retrieval APIs, or domain databases (e.g.,  
 715 scholarly indices, code search). Let an external retriever implement a (possibly stochastic) mapping  
 716  $\mathcal{R} : (q, s) \mapsto r$ , where  $q$  is a query issued by the LLM and  $s$  is the (latent) world/index state at the  
 717 time of the call. Even when  $\mathcal{R}$  is not perfectly deterministic, the *trajectory* that includes the returned  
 718 snippet  $r$  is unreachable for a pure-text model unless it *guesses* the salient facts in  $r$  token-by-token.  
 719 This mirrors the random-oracle argument in Theorem 3.4: as the entropy of  $r$  conditioned on  $(q, x)$   
 720 grows, the probability that a pure-text model reproduces  $r$  by chance decays exponentially, while a  
 721 tool-augmented model obtains  $r$  via a single call. Hence support expands, and under any fixed budget  
 722  $B$  the feasible set also strictly expands once the text-only paraphrase of  $r$  would exceed  $B$ .

723 **Checkers, Verifiers, and Program Runners.** Beyond “heavy” computation, many tools act as  
 724 *verifiers*: unit tests, symbolic algebra checkers, SAT/SMT solvers, theorem provers, type checkers,  
 725 or even a Python REPL used only to validate a candidate answer. Such tools add *deterministic  
 726 pruning* transitions to the trajectory graph: incorrect branches are cut immediately with  $O(1)$  tokens.  
 727 This reduces the exploration burden under RLVR-style training and enlarges the set of practically  
 728 reachable strategies under a budget.

729 **Stateful External Memory.** Tools can expose memory larger and more persistent than the model’s  
 730 context: key-value caches, external scratchpads, vector stores, or file systems. Each call updates an  
 731 external state  $m_{t+1} = U(m_t, a_t)$  and reads views  $v_t = V(m_t)$  at  $O(1)$  token cost. Strategies that  
 732 require memory  $|m| \gg B$  are impossible to realize faithfully in pure text (which must inline  $m$ ), but  
 733 become feasible when memory lives outside the context window.

734 **Proposition E.1** (Informal; External State as Unbounded Scratchpad). *Suppose an algorithm requires  
 735  $\Omega(n)$  writable memory cells for problem size  $n$ . If a tool exposes these cells with per-step I/O  
 736  $O(1)$ , then for sufficiently large  $n$ , the algorithm’s equivalence class lies in  $\text{supp}_B(p_{\text{TIR}})$  but not in  
 737  $\text{supp}_B(q_{\text{text}})$  for any fixed  $B$ .*

738 **Embodied and Interactive Environments.** When the LLM acts in an MDP or game environment  
 739 (Xu et al., 2025), the environment transition  $s_{t+1} = E(s_t, a_t)$  is itself an *external oracle*. Our  
 740 earlier support-expansion argument applies verbatim: trajectories that include specific environment  
 741 observations or states are unreachable by text-only generation unless they are guessed token-by-  
 742 token. Token-efficiency arguments also lift: environment interactions can realize long-horizon plans  
 743 with *summarized* textual traces, whereas a pure-text simulation would require enumerating each  
 744 counterfactual step.

745 **Noisy or Non-Deterministic Tools.** Stochastic returns (e.g., fluctuating search rankings) do not  
 746 invalidate support expansion. What matters is the existence of *some* positive-probability outputs with  
 747 substantial conditional entropy that are infeasible to reproduce via text within budget. In other words,  
 748 determinism is a convenience, not a necessity, for our conclusions.

750 **Composing Multiple Tools.** Real agents chain retrieval, computation, verification, and environment  
 751 actions. Composition behaves monotonically:

752 **Proposition E.2** (Informal; Monotone Closure under Composition). *Let  $\mathcal{T}_1, \dots, \mathcal{T}_k$  be tools with  
 753 per-call costs that sum to at most  $B$ . If each  $\mathcal{T}_i$  individually yields a strict feasible-support gain  
 754 for some subproblem family at size  $n_i$ , then there exist composite tasks for which the sequential (or  
 755 branched) use of  $\{\mathcal{T}_i\}$  yields a strict feasible-support gain over any pure-text policy at the same total  
 budget.*

756  
 757 **Takeaway.** “Python” is merely one instantiation of a broader principle, our extensions unify code  
 758 execution, search, verification, memory, and embodied interaction under the same analytical lens.  
 759  
 760  
 761

## 762 F EXAMPLES ON TOKEN EFFICIENCY

763  
 764  
 765  
 766  
 767 Table 1: Contrasting Token Efficiency for an Iterative Task ( $N \rightarrow \infty$ )  
 768

769 770 <b>Programmatic Approach (Python)</b>	771 <b>Natural Language Reasoning</b>
771 A symbolic, abstract representation of the computation. The token cost is constant and independent of $N$ . 772 773	771 A concrete, step-by-step enumeration of the computation. The token cost scales with the magnitude of $N$ . 772 773
774 775 1 # N can be 10,000,000 or more 776 2 for i in range(N): 777 3 # Perform some check 778 4 check(i) 779 780 781 782 783	774 775 <i>”Okay, to solve this, I must check every number. First, for n=1, I perform the check... Next, for n=2, I perform the check... Next, for n=3, I perform the check... ... (This enumeration continues for millions of steps) ... Finally, for n=10,000,000, I perform the check...”</i> 776 777 778 779 780 781 782 783

784  
 785 Table 2: Contrasting Token Efficiency for Solving Large Linear Systems  
 786  
 787  
 788  
 789  
 790  
 791  
 792

793 794 <b>Programmatic Approach (Python)</b>	795 <b>Natural Language Reasoning</b>
795 A single call to a highly optimized numerical library solves $Ax = b$ . The token cost is constant, independent of the matrix dimension $n$ . 796 797 798	795 A detailed explanation of Gaussian elimination, requiring a description of each row operation. The token cost scales with the matrix size. 796 797 798
800 801 1 import numpy as np 802 2 # A is a large n x n matrix, 803 3 # e.g., n=1000 804 4 x = np.linalg.solve(A, b) 805 806 807 808 809	800 801 <i>”To solve the system, we perform Gaussian elimination. First, to eliminate the first variable from the second row, we subtract <math>A_{2,1}/A_{1,1}</math> times the first row from the second row. We must do this for all <math>n - 1</math> rows below the first. Next, we use the new second row to eliminate the second variable from the rows below it... (This narration continues for <math>O(n^2)</math> elements and <math>O(n^3)</math> operations.)”</i> 802 803 804 805 806 807 808 809

809 **Token Cost:** A few tokens. Scales as  $O(1)$ . Enables solving massive systems within a tiny token budget.

809 **Token Cost:** Proportional to the number of elements in the matrix to sketch. Scales as  $\Omega(n^2)$ . A full narration would scale as  $\Omega(n^3)$ .

810 Table 3: Contrasting Token Efficiency for a Dynamic Programming Task (Fibonacci Sequence)  
811

812 <b>Programmatic Approach (Python)</b>	813 <b>Natural Language Reasoning</b>
814 A compact representation of the recurrence relation, with a token cost independent of the input integer $N$ .	815 A verbose, step-by-step calculation of every subproblem’s solution, with a token cost that grows with $N$ .
816	817
818 1 memo = {0: 0, 1: 1} 819 2 def fib(n): 820 3 if n in memo: return memo[n] 821 4 memo[n] = fib(n-1) + fib(n-2) 822 5 return memo[n]	823 <i>"To get fib(5), I need fib(4) and fib(3). Fib(2) is fib(1)+fib(0) = 1+0 = 1. Fib(3) is fib(2)+fib(1) = 1+1 = 2. Fib(4) is fib(3)+fib(2) = 3+1 = 4. So, fib(5) is fib(4)+fib(3) = 4+2 = 6... Wait, let me recheck. fib(4) is 3+2=5. No, fib(4) is 2+1=3. Okay, so fib(5) is 3+2=5."</i>
824 <b>Token Cost: <math>O(1)</math></b>	825 <b>Token Cost: <math>\Omega(N)</math></b>

826 Table 4: Contrasting Token Efficiency for Search Algorithms  
827

828 <b>Programmatic Approach (Python)</b>	829 <b>Natural Language Reasoning</b>
830 An abstract procedure for state-space traversal, using data structures like a queue and a set.	831 A full, step-by-step narration of the entire exploration process, including every node visited and every state change of the queue.
832	833
834 1 from collections import deque 835 2 836 3 def bfs(graph, start_node): 837 4 queue = deque([start_node]) 838 5 visited = {start_node} 839 6 while queue: 840 7 node = queue.popleft() 841 8 # Process node 842 9 for neighbor in graph[node]: 843 10 if neighbor not in visited 844 11 : 845 12 visited.add(neighbor) 846 13 queue.append(neighbor)	834 <i>"I start at node 'A'. Queue is ['A'], visited is 'A'. I pop 'A'. Its neighbors are 'B', 'C'. Queue is now ['B', 'C'], visited is 'A','B','C'. I pop 'B'. Its neighbor is 'D'. Queue is now ['C', 'D'], visited is 'A','B','C','D'. I pop 'C'..." (and so on)</i>
847 <b>Token Cost:</b> Constant cost for the algorithm’s definition. Scales as $O(1)$ .	848 <b>Token Cost:</b> Proportional to the number of vertices and edges, $V + E$ . Scales as $\Omega(V + E)$ .

849  
850 **G ANALYSIS OF THE FAILED REWARD-BASED APPROACH**851  
852 To encourage the earlier code invocation, our initial and most direct approach was to introduce an  
853 *early-code reward* directly into the reward function. For each response  $i$  that is both correct and  
854 code-containing in a group of samples, we added a reward term  $r'_i$  that penalizes later code invocation:  
855

856  
857 
$$R_i = 1 + r'_i \quad \text{where} \quad r'_i = \delta \cdot \text{clip} \left( \frac{p_i - \text{mean}(\mathbf{p})}{\text{std}(\mathbf{p})}, -c, c \right).$$
  
858

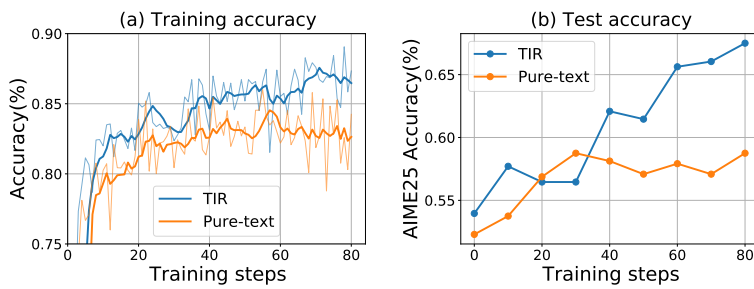
859 where  $\mathbf{p}$  is the set of first code invocation positions for all correct, code-containing responses within  
860 the group. Furthermore,  $\delta$  is a negative coefficient to encourage early code invocation, and  $c$  is  
861 a clipping hyperparameter. However, this seemingly innocuous modification proved to be highly  
862 destabilizing during training (see experimental details in Section 4.4 and Figure 3 (a)). In algorithms  
863 like GRPO that rely on group normalized advantage, this design has a critical flaw. In the common  
864 scenario where all samples in a group are correct, the primary reward signal (the constant ‘1’) is

864 entirely eliminated by the normalization. The advantage calculation then becomes:  
 865

$$866 A_i = \frac{R_i - \text{mean}(\mathbf{R})}{\text{std}(\mathbf{R})} = \frac{(1 + r'_i) - (1 + \text{mean}(\mathbf{r}'))}{\text{std}(\mathbf{r}')} = \frac{r'_i - \text{mean}(\mathbf{r}')}{\text{std}(\mathbf{r}')}$$

868 This leads to a catastrophic outcome: (1) the primary signal about answer correctness disappears,  
 869 (2) the auxiliary signal  $r'_i$  is amplified to the same magnitude as the original primary signal, and (3)  
 870 due to the nature of standardization, approximately half of these correct responses receive a negative  
 871 advantage and are thus heavily penalized, solely because their code invocation is later than the group's  
 872 average.  
 873

## 874 H EXPERIMENTAL SETUP



886 Figure 5: The (a) training and (b) testing accuracy of the TIR and pure-text RL on Qwen3-8B model.  
 887 The AIME25 accuracy (b) is the average of 16 responses.  
 888

889 **Model and Datasets.** All experiments are based on the Qwen3-8B model (Qwen, 2025). For our  
 890 training data, we randomly sample 10,000 English problems from the DAPO dataset (Yu et al., 2025)  
 891 due to limited computational resources. Since our aim is to fundamentally understand the mechanisms  
 892 of TIR *rather than* to improve absolute accuracy of benchmarks, this dataset is sufficient for our  
 893 purpose, in contrast to the extensive training datasets used in other literature (Yu et al., 2025; Feng  
 894 et al., 2025). Our primary evaluation benchmarks are AIME24, AIME25, and a challenging subset of  
 895 the Omni-MATH dataset (Gao et al., 2024). For the latter, due to the large size of the dataset, we  
 896 curated the 512 *most difficult* problems that are amenable to reliable, rule-based evaluation, which  
 897 we denote as Omni-MATH-512. **While AIME-style problems have numerical final answers, Omni-**  
 898 **MATH-512 contains a substantial fraction of problems whose final answers are symbolic expressions**  
 899 **rather than single numbers. Together with the large answer space (000–999 for AIME, symbolic**  
 900 **expressions for part of Omni-MATH-512), this makes blind guessing an implausible explanation for**  
 901 **the observed gains.**

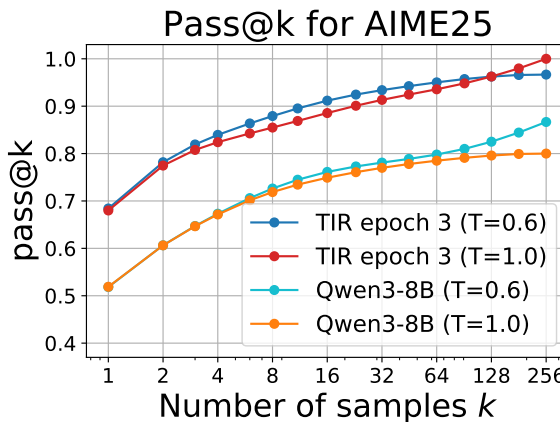
902 **Training Protocol.** We train two main models for comparison: our proposed TIR model, which can  
 903 execute code to assist in its reasoning process, and a pure-text RL model as a baseline (as shown in  
 904 Figure 5). Both models are trained for 3 epochs using the DAPO algorithm (Yu et al., 2025), a variant  
 905 of GRPO (DeepSeek, 2025), **with the same dataset and hyperparameters; the only difference is an**  
 906 **additional system prompt that specifies the tool usage format for the TIR model.** During training, we  
 907 use a rollout batch size of 96 problems, with 8 responses sampled per problem, a maximum response  
 908 length of 16,384 tokens, and a sampling temperature of 1.0 to encourage exploration.

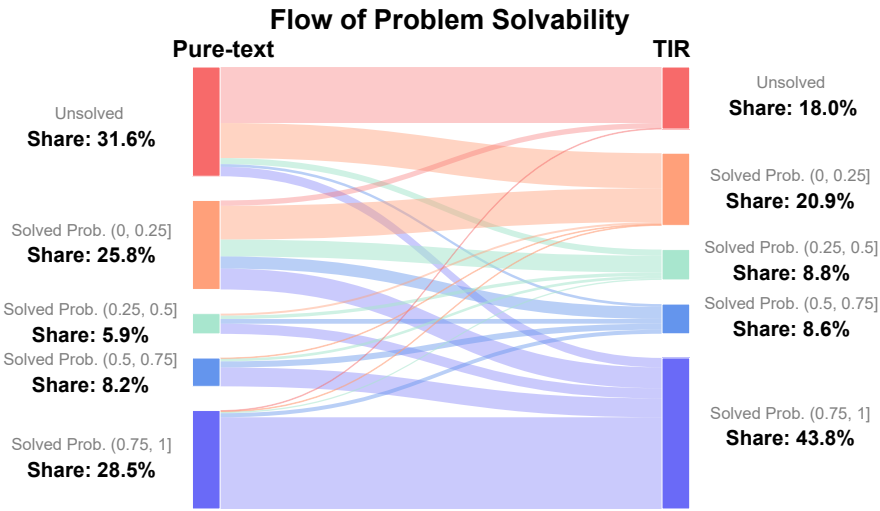
909 **Evaluation Protocol.** For evaluations, we set the sampling temperature to 0.6 and maximum response  
 910 length to 16,384 tokens unless otherwise specified.

911 **To avoid overclaiming, we explicitly clarify the scope of our experimental setup. Our experiments**  
 912 **focus on a single tool (Python interpreter), a single model family (Qwen3-8B), and mathematical**  
 913 **reasoning tasks. This design choice is motivated by the goal of isolating and interpreting the core**  
 914 **mechanisms of Tool-Integrated Reasoning, rather than benchmarking a broad set of tools or domains.**  
 915 **Python provides a deterministic, high-information-density computational interface that allows us**  
 916 **to cleanly analyze support expansion. Although we do not empirically test other tools, Appendix E**  
 917 **discusses how our theoretical arguments extend to a broad family of external tools. We leave**  
 918 **multi-tool, multi-domain evaluations to future work.**

918 **I PASS@ $k$  DATA**  
919920 Table 5 shows the detailed pass@ $k$  results for the TIR and pure-text models across the three benchmarks,  
921 evaluated with the max sample size of 256.  
922923 Table 5: Pass@ $k$  results for the TIR model and the pure text model  
924

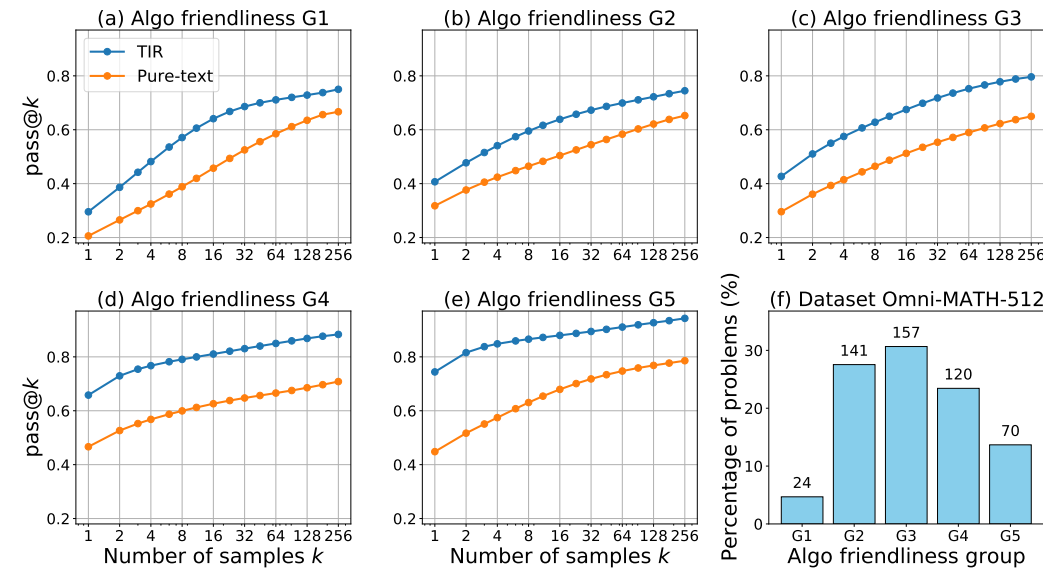
k	AIME24		AIME25		Omni-MATH-512	
	TIR	Pure Text	TIR	Pure Text	TIR	Pure Text
1	0.7829	0.6331	0.6841	0.5184	0.5128	0.3585
2	0.8408	0.7184	0.7818	0.6065	0.5885	0.4208
4	0.8632	0.7703	0.8395	0.6730	0.6437	0.4707
8	0.8825	0.8050	0.8792	0.7262	0.6869	0.5153
16	0.9024	0.8312	0.9117	0.7613	0.7232	0.5570
32	0.9173	0.8496	0.9339	0.7810	0.7545	0.5942
64	0.9312	0.8645	0.9503	0.7979	0.7802	0.6271
128	0.9480	0.8813	0.9625	0.8250	0.8018	0.6575
256	0.9667	0.9000	0.9667	0.8667	0.8203	0.6836

938 **J TEMPERATURE SENSITIVITY ANALYSIS**  
939955 Figure 6: Pass@ $k$  curves on AIME25 under temperatures 0.6 and 1.0 for the TIR (RL trained) and  
956 pure-text models (Qwen3-8B) model.  
957958 To examine whether our conclusions depend on sampling temperature, we measured pass@ $k$  on  
959 AIME25 under temperatures 0.6 and 1.0 for both TIR and pure-text model, as shown in Figure 6.  
960 For small  $k$ , both models show almost identical pass@ $k$  curves across temperatures. For large  $k$ ,  
961 increasing the temperature to 1.0 increases the diversity of TIR trajectories and slightly improves  
962 its tail-end pass@ $k$ . In contrast, the pure-text model becomes noticeably noisier under temperature  
963 1.0, resulting in lower pass@256. This phenomenon is consistent with prior observations in  
964 Yue et al. (2025), which reports that the base model drops but the RL-trained model remains stable when  
965 temperature exceeds 1.0.  
966967 Across temperatures, the TIR model consistently outperforms the pure-text model. This supports our  
968 core claim that TIR's gains stem from structural support expansion, rather than sampling stochasticity.  
969  
970

972 **K CAPABILITY EXPANSION AND SHRINKAGE**  
973  
974  
975  
976  
977  
978  
979  
980  
981  
982  
983  
984  
985  
986  
987  
988  
989  
990  
991  
992993 Figure 7: The detailed flow of problem solvability on Omni-MATH-512 when transitioning from the  
994 pure-text model to the TIR model. The solved probability of each problem is evaluated at  $k = 256$ .  
995  
996997 **L ANALYSIS OF THE 1.8% CAPABILITY SHRINKAGE**  
998  
9991000 To better understand the small “capability shrinkage” observed in Figure 2, where the TIR model fails  
1001 on 9 problems that the pure-text model solves, we conducted a detailed item-level analysis. Across  
1002 512 evaluated problems, shrinkage occurs in 9 cases (1.8%), which is substantially smaller than the  
1003 gain in newly solved problems (+15.4%). Below we show that the shrinkage is either attributable to  
1004 sampling variance or to RL training artifacts, rather than an inherent limitation of TIR.  
10051006 **1.** For 6 of the 9 problems, the pure-text model solved them only 1 or 2 times out of 256 samples, while  
1007 the TIR model solved them 0 times. These problems have extremely low base success probabilities,  
1008 and a shift from 1–2 correct samples to 0 correct samples is fully explainable by Monte-Carlo variance.  
1009 So these cases do not reflect a meaningful capability shrinkage.  
10101011 **2.** The remaining 3 problems exhibit larger drops. To determine whether this is caused by TIR or  
1012 by RL training, we evaluated a non-RL TIR model (vanilla Qwen3-8B + Python tool, no RL fine-  
1013 tuning) on these 3 problems. This model preserved the pure-text model’s accuracy on all 3 problems,  
1014 indicating that the drops were introduced by RL, not by the TIR mechanism itself. This aligns with  
1015 prior observations that RL can occasionally induce forgetting and cause capability shrinkage (Yue  
1016 et al., 2025; Wu et al., 2025).  
10171018 Thus, the 1.8% shrinkage should be interpreted as: A small, explainable artifact of RL fine-tuning  
1019 and sampling variance, rather than a limitation of TIR. This complements our main result that TIR  
1020 achieves large support expansion (+15.4% newly solved problems), far outweighing these minor,  
1021 non-inherent shrinkage effects.  
1022  
1023  
1024  
1025

1026 **M RUBRIC FOR ALGORITHMIC FRIENDLINESS**  
10271028 Table 6 shows the rubric we use for Gemini Pro APIs (Gemini, 2025) to classify the math problems.  
10291030 Table 6: Rubric for assessing the “algorithmic friendliness” of problems.  
1031

Score	Level	Description	Required Insight
5	<b>Very High</b> (Direct Application)	The problem is a textbook example for a standard algorithm (e.g., backtracking). The problem statement itself almost serves as the specification. <b>Almost no mathematical insight is needed.</b>	None beyond basic arithmetic.
4	<b>High</b> (Minor Insight)	An algorithm provides a clear advantage, but requires a <b>standard, well-known mathematical identity</b> or <b>simple transformation</b> to be applied. The mathematical hurdle is low.	Recalling and applying a common formula or theorem.
3	<b>Medium</b> (Significant Insight)	A computational solution is effective, but only after applying a <b>significant mathematical insight</b> or performing <b>complex problem modeling</b> . The difficulty is substantial.	A creative, problem-specific trick or a complex modeling effort.
2	<b>Low</b> (Impractical Algorithm)	An algorithm is theoretically possible but highly impractical (enormous search space, precision issues). The algorithmic optimizations are <b>equivalent in difficulty to the mathematical solution.</b>	Insights needed are essentially the mathematical solution itself.
1	<b>Very Low</b> (Non-computational)	The problem is fundamentally abstract and cannot be solved by computation (e.g., requires a formal proof, deals with uncountable sets).	N/A.

1080 N PASS@ $k$  CURVES FOR PROBLEMS GROUPED BY ALGO FRIENDLINESS  
1081

1101 Figure 8: (a)-(e) Pass@ $k$  curves for the TIR and pure-text models, grouped by problem algo  
1102 friendliness. (f) The distribution of algo friendliness scores across the Omni-MATH-512 dataset.  
1103 The problems are categorized into five groups based on their algo friendliness scores: 1.0–1.5 (G1),  
1104 2.0–2.5 (G2), 3.0–3.5 (G3), 4.0–4.5 (G4), and 5.0 (G5).

1105  
1106  
1107  
1108  
1109  
1110  
1111  
1112  
1113  
1114  
1115  
1116  
1117  
1118  
1119  
1120  
1121  
1122  
1123  
1124  
1125  
1126  
1127  
1128  
1129  
1130  
1131  
1132  
1133

---

## 1134 O EMERGENT COGNITIVE PATTERNS OF TOOL INTEGRATION

1136 The quantitative results of the previous sections demonstrate *that* TIR is universally effective, but  
 1137 they do not fully explain *how*. If the model’s advantage is not limited to algorithmically amenable  
 1138 problems, how exactly is it leveraging the code interpreter to solve problems requiring abstract  
 1139 insight? Through qualitative analysis of model outputs, we have identified three distinct and recurring  
 1140 patterns of code utilization that answer this question.

1141 **Pattern 1: Insight-to-computation transformation.** In this primary pattern, the model’s first  
 1142 step is not to code, but to *reason*. It engages in non-trivial, text-based analysis to deconstruct a  
 1143 complex problem, applying mathematical insights to transform it into a state that is amenable to a  
 1144 programmatic solution. The code interpreter is then invoked to execute a genuine algorithm (such  
 1145 as search, enumeration, or DP) that efficiently solves this newly formulated sub-problem under a  
 1146 limited computational resource. Unlike straightforward sequential calculations one might perform  
 1147 with a calculator, these algorithms often possess complex control flows (e.g., loops, recursion) that  
 1148 are challenging for a language model to emulate or follow step-by-step.

1149 For instance, as shown in Table 7, the model first uses mathematical reasoning to derive a transcendental  
 1150 equation from the abstract geometric problem. It then employs code to iterate the entire parameter  
 1151 space of  $(m, n)$  pairs, using the Intermediate Value Theorem as a numerical method to efficiently  
 1152 detect whether a solution exists for each pair.

1153 **Table 7: A case of insight-to-computation transformation.**

---

1155 **[Question]**

1156 Let  $a \neq b$  be positive real numbers and  $m, n$  be positive integers. An  $m + n$ -gon  $P$  has the property that  $m$   
 1157 sides have length  $a$  and  $n$  sides have length  $b$ . Further suppose that  $P$  can be inscribed in a circle of radius  
 1158  $a + b$ . Compute the number of ordered pairs  $(m, n)$ , with  $m, n \leq 100$ , for which such a polygon  $P$  exists for  
 1159 some distinct values of  $a$  and  $b$ .

1160 **[Response]**

1161 Okay, let’s try to tackle this problem step by step.

1162 ...  
 1163 We need to find the number of ordered pairs  $(m, n)$  where  $m, n \leq 100$  such that this equation has solutions  
 1164 for  $a$  and  $b$  with  $a \neq b$ . ... So, substituting into the equation:

$$1165 \quad m \cdot \arcsin(x/2) + n \cdot \arcsin((1-x)/2) = \pi$$

1166 ...  
 1167 But how can I find all such  $(m, n)$  pairs? Since  $m$  and  $n$  are up to 100, perhaps we can write a program to  
 1168 check for each possible pair  $(m, n)$  whether there exists an  $x$  in  $(0, 1)$  such that the equation is satisfied.  
 1169 But how to implement this check in Python? The problem is that the equation is transcendental and might  
 1170 not have an analytical solution, so numerical methods would be needed. For each  $(m, n)$ , we can define a  
 1171 function  $f(x) = m \cdot \arcsin(x/2) + n \cdot \arcsin((1-x)/2) - \pi$ , and check if there’s a root of  $f(x) = 0$   
 1172 in  $(0, 1)$ , excluding  $x = 0.5$ . But how to check for roots? For example, we can use the Intermediate Value  
 1173 Theorem. If  $f(x)$  changes sign over an interval, there’s a root in that interval.

1174 ...  
 1175 Now, let’s proceed to write the Python code.

1176 <code>

```
1177 import math
1178
1179 def has_solution(m, n):
1180     def f(x):
1181         return m * math.asin(x/2) + n * math.asin((1 - x)/2) - math.pi
1182
1183     # Check interval (0, 0.5)
1184     left = 0.0001
1185     right = 0.4999
1186     if f(left) * f(right) < 0:
1187         return True
1188
1189     # Check interval (0.5, 1)
```

```

1188
1189     14     left = 0.5001
1190     15     right = 0.9999
1191     16     if f(left) * f(right) < 0:
1192     17         return True
1193     18
1194     19     return False
1195
1196     21 count = 0
1197     22 for m in range(1, 101):
1198     23     for n in range(1, 101):
1199     24         if has_solution(m, n):
1200     25             count += 1
1201
1202     27 print(count)
1203
1204     28 
```

&lt;/code&gt;

&lt;interpreter&gt; 940 &lt;/interpreter&gt;

...

1205 Wait, but the code is written in Python, and the interpreter output is 940. So the final answer is 940.

1206

1207

1208

1209

1210 **Pattern 2: Exploration and verification via code.** For problems where the solution path is not immediately obvious, the model utilizes the code interpreter as an interactive sandbox for exploration and hypothesis testing. Instead of committing to a *single line* of reasoning, it formulates conjectures and writes short code snippets to test them, observe their outcomes, and iteratively refine its strategy based on the feedback. This pattern is particularly prevalent in problems with low algorithmic amenability, where it allows the model to build confidence and discover insights through empirical experimentation.

1211 Table 8 provides a clear instance of pattern 2: exploration and verification via code. The model first

1212 derives a candidate value of  $\lambda = \sqrt{3}$  from a simple case, then uses the code interpreter to numerically

1213 explore more different scenarios. The feedbacks validate its initial hypothesis and pivot its strategy

1214 from further exploration toward constructing a rigorous algebraic proof.

1215 These first two patterns represent a fundamental departure from pure-text reasoning. As we established

1216 in Section 3, they constitute entirely new *Computational Equivalence Classes*, new strategies for

1217 solving problems. While a pure-text model might theoretically be able to simulate these processes,

1218 the token cost of doing so would be astronomical. The step-by-step, trial-and-error nature of the

1219 exploratory pattern, in particular, would lead to a blow-up in token length. Therefore, these strategies

1220 lie far outside the *Feasible Support under Budget B* for any practical context window, making them

1221 uniquely accessible to the TIR paradigm.

1222 Table 8: A case of exploration and verification via code.

1223 **[Question]**

1224 Find the largest real number  $\lambda$  with the following property: for any positive real numbers  $p, q, r, s$  there exists

1225 a complex number  $z = a + bi$  ( $a, b \in \mathbb{R}$ ) such that

$$1226 |b| \geq \lambda|a| \quad \text{and} \quad (pz^3 + 2qz^2 + 2rz + s) \cdot (qz^3 + 2pz^2 + 2sz + r) = 0.$$

1227 **[Response]**

1228 Okay, let's try to tackle this problem step by step.....

1229 But how do we approach this? Maybe we can think about the problem by considering specific cases ... Perhaps

1230 the worst case occurs when  $p = q$  and  $r = s$ ? ... Let's try to consider a symmetric case. ... Maybe choosing

1231  $p = q = 1$  and  $r = s = 1$ . Let's try that. ...

1232 The roots are  $z = -1$  and roots of  $z^2 + z + 1 = 0$ , which are  $\frac{-1 \pm i\sqrt{3}}{2}$ . Let's compute their  $|b|/|a|$ :

$$1233 z = \frac{-1 \pm i\sqrt{3}}{2} \rightarrow a = -1/2, b = \pm\sqrt{3}/2.$$

1242  
 1243 So  $|b| = \sqrt{3}/2$ ,  $|a| = 1/2$ . So  $|b|/|a|$  is  $\sqrt{3}$ .  
 1244 So for this case,  $\lambda$  can be as large as  $\sqrt{3}$ . But this is just for this specific case. ...  
 1245 This is getting a bit abstract. Maybe we can consider a case where both  $P(z)$  and  $Q(z)$  have roots with  
 1246 minimal  $|b|/|a|$ , and find what that value is. ... when  $t$  is very small. Let me try to find its roots numerically  
 1247 for a specific small  $t$ . Let me write a Python code snippet to find the roots of  $P(z) = z^3 + 2z^2 + 0.2z + 0.1$ .  
 1248 `<code>`  
 1249 

```
1 import numpy as np
2
3 # Coefficients for P(z) = z^3 + 2z^2 + 0.2z + 0.1
4 coeffs = [1, 2, 0.2, 0.1]
5 roots = np.roots(coeffs)
6 print(roots)
7
```

  
 1255 `</code>`  
 1256 `<interpreter>` [-1.92303902+0.j, -0.03848049+0.22476716j, -0.03848049-0.22476716j]  
 1257 `</interpreter>`  
 1258 For these complex roots,  $|b|/|a|$  is  $0.2248/0.0385 \approx 5.83$ . ... Wait, but this case gives a high value of  $|b|/|a|$ .  
 1259 So maybe the worst case is when the minimal such value is low. ...  
 1260 But how to find that? It seems challenging without more insight. ... Alternatively, consider using symmetry.  
 1261 ... But if we set  $s = 4qr/p$ , for example, let's set  $p = 1, q = 1, r = 1$ , then  $s = 4 * 1 * 1/1 = 4$ . So  
 1262  $P(z) = z^3 + 2z^2 + 2z + 4$ . Let's find its roots. Using numpy again:  
 1263 `<code>`  
 1264 

```
1 import numpy as np
2
3 coeffs = [1, 2, 2, 4]
4 roots = np.roots(coeffs)
5 print(roots)
6
```

  
 1270 `</code>`  
 1271 `<interpreter>` [-2.00000000e+00+0.j, 1.66533454e-16+1.41421356j, 1.66533454e-16-1.41421356j]  
 1272 `</interpreter>`  
 1273 So  $|b|/|a|$  is infinite (since  $a$  is nearly zero), but for practical purposes, this suggests that for this case, there  
 1274 are roots with very large  $|b|/|a|$ . So this case is not helpful. ... This suggests that for this case, we can achieve  
 1275  $|b|/|a|$  up to  $\sqrt{3}$ .  
 1276 ...  
 1277 Let's think of a case where the ratio is lower than  $\sqrt{3}$ . ... Let me consider the case where  $p = q = 1, r = 1, s = 2$ . Then  $P(z) = z^3 + 2z^2 + 2z + 2$ . Let's find its roots using numpy.  
 1278 `<code>`  
 1279 

```
1 import numpy as np
2
3 coeffs = [1, 2, 2, 2]
4 roots = np.roots(coeffs)
5 print(roots)
6
```

  
 1286 `</code>`  
 1287 `<interpreter>` [-1.54368901+0.j, -0.22815549+1.11514251j, -0.22815549-1.11514251j]  
 1288 `</interpreter>`  
 1289 So  $|b|/|a| = 1.115/0.228 \approx 4.89$ . The real root has  $|b|/|a| = 0$ . So again, the maximum is 4.89.  
 1290 This doesn't seem to help. ... Let me think of a different approach. ...  
 1291 Let me assume that there is a root  $z = a + bi$  with  $|b| = \lambda|a|$ . Let's assume  $a \neq 0$ . Then,  $b = \lambda a$  or  $b = -\lambda a$ .  
 1292 Let's assume  $b = \lambda a$ . ... Substitute  $z = a + \lambda ai = a(1 + \lambda i)$  into  $P(z) = pz^3 + 2qz^2 + 2rz + s = 0$ .  
 1293 ...  
 1294 Since  $a \neq 0$  and  $\lambda$  is non-zero (otherwise, we have real roots), we can divide both sides by  $\lambda a$ :  
 1295 
$$pa^2(3 - \lambda^2) + 4qa + 2r = 0$$

1296

1297 This is one equation.

1298 From the equation, since all terms except the first are positive, we must have  $(3 - \lambda^2) < 0$ , which implies  
1299  $\lambda^2 > 3$ , or  $\lambda > \sqrt{3}$ . This suggests that for *any* non-real root, the ratio  $|b|/|a|$  must be greater than  $\sqrt{3}$ .

1300

1301 So, we have two key pieces of information:

1302

1. We found a specific case ( $p = q = r = s = 1$ ) where the largest available ratio is exactly  $\sqrt{3}$ . This means  $\lambda$  cannot be greater than  $\sqrt{3}$ .
2. Our general proof shows that for any case with a non-real root, the ratio must be greater than or equal to  $\sqrt{3}$ . This means  $\lambda$  must be at least  $\sqrt{3}$ .

1303

1304 Combining these, the largest possible value for  $\lambda$  is exactly  $\boxed{\sqrt{3}}$ .

1305

1306

1307

1308

1309

1310

1311

1312

**Pattern 3: Offloading complex calculation.** This is the most direct pattern of tool use, where the model has a clear, linear path to the solution but delegates complex or tedious calculations to the interpreter. This usage aligns with the naive view of TIR as a “calculator”, but its importance should not be understated. By offloading these steps, the model minimizes the *risk* of unforced computational errors that frequently derail long chains of pure-text thought, thereby preserving the integrity of the overall reasoning process.

1313

1314

1315

1316

1317

1318

1319

1320

1321

1322

1323

1324

1325

1326

1327

A representative example is shown in Table 9. Here, the model first performs the text-based reasoning to establish a solution path, then uses the interpreter as a precision tool to execute the series of intricate vector and algebraic computations that would be highly prone to manual error. In conclusion, these emergent patterns reveal a sophisticated interplay between the LLM’s reasoning capabilities and the code interpreter’s computational power. The model is not merely using a tool; it is *thinking with tools*. This signifies a fundamental shift in strategy: rather than simply delegating calculations from an otherwise unchanged, text-based line of thought, the model learns to generate novel problem-solving approaches that are intrinsically synergistic with the interpreter. It formulates plans that leverage programmatic strengths like iteration and DP from the outset, developing new “Computational Equivalence Classes” that were previously inaccessible. Such dynamic and flexible code invocation enables the TIR model to break the capability ceiling of its pure-text counterpart.

1328

Table 9: A case of offloading complex calculation.

1329

1330

1331

**[Question]**  
Let acute triangle  $ABC$  have circumcenter  $O$ , and let  $M$  be the midpoint of  $BC$ . Let  $P$  be the unique point such that  $\angle BAP = \angle CAM$ ,  $\angle CAP = \angle BAM$ , and  $\angle APO = 90^\circ$ . If  $AO = 53$ ,  $OM = 28$ , and  $AM = 75$ , compute the perimeter of  $\triangle BPC$ .

1332

1333

1334

**[Response]**

Okay, let’s try to solve this problem step by step.

1335

1336

1337

Alternatively, maybe using coordinate geometry. Let me think about setting up coordinates.

1338

1339

First, compute  $A_x$ ,  $A_y$  numerically.

1340

1341

$$A_x = (75\sqrt{13})/7, \quad A_y = 450/7$$

1342

1343

Then compute vectors  $AB$  and  $AC$ , their lengths, unit vectors, angle bisector direction, then reflect  $AM$  over this direction to get the direction of  $AP$ . Then find the intersection of this line with the circle.

1344

But implementing all this in code is time-consuming, but let’s try. Let me write the code.

1345

`<code>`

1346

1347

1348

1349

```
1 import math
2
3 # Given values
4 AO = 53
```

```

1350
1351     5 OM = 28
1352     6 AM = 75
1353
1354     8 # Compute Ay
1355     9 Ay = 450 / 7
1356    10 # Compute Ax
1357    11 sqrt13 = math.sqrt(13)
1358    12 Ax = (75 * sqrt13) / 7
1359
1360    14 # Coordinates of A
1361    15 A = (Ax, Ay)
1362    16 # Coordinates of O
1363    17 O = (0, 28)
1364    18 # Coordinates of M
1365    19 M = (0, 0)
1366    20 # Coordinates of B and C
1367    21 B = (-45, 0)
1368    22 C = (45, 0)
1369
1370
1371    24 # Function to compute vector from point1 to point2
1372    25 def vector(p1, p2):
1373        26     return (p2[0] - p1[0], p2[1] - p1[1])
1374
1375
1376    28 # Compute vectors AB and AC
1377    29 AB = vector(A, B)
1378    30 AC = vector(A, C)
1379
1380
1381    32 # Compute lengths of AB and AC
1382    33 len_AB = math.hypot(AB[0], AB[1])
1383    34 len_AC = math.hypot(AC[0], AC[1])
1384
1385
1386    36 # Compute unit vectors
1387    37 unit_AB = (AB[0]/len_AB, AB[1]/len_AB)
1388    38 unit_AC = (AC[0]/len_AC, AC[1]/len_AC)
1389
1390
1391    40 # Angle bisector direction
1392    41 angle_bisector_dir = (unit_AB[0] + unit_AC[0], unit_AB[1] + unit_AC
1393        42 [1])
1394
1395
1396    43 # Vector AM
1397    44 AM_vec = vector(A, M)
1398
1399
1400    46 # Function to reflect a vector over another vector
1401    47 def reflect_vector(v, axis):
1402        48     # Normalize the axis vector
1403        49     axis_len = math.hypot(axis[0], axis[1])
1404        50     if axis_len == 0:
1405        51         return v
1406        52     axis_unit = (axis[0]/axis_len, axis[1]/axis_len)
1407
1408
1409    54 # Dot product
1410    55     dot = v[0] * axis_unit[0] + v[1] * axis_unit[1]
1411
1412
1413    57 # Projection of v onto axis
1414    58     proj = (dot * axis_unit[0], dot * axis_unit[1])
1415
1416
1417    60 # Reflection
1418    61     reflected = (2*dot*axis_unit[0] - v[0], 2*dot*axis_unit[1] - v[1])
1419
1420    62     return reflected
1421
1422
1423    64 # Reflect AM_vec over angle bisector direction
1424    65     AP_dir = reflect_vector(AM_vec, angle_bisector_dir)
1425
1426

```

```

1404
1405     # Normalize AP_dir to get direction
1406     AP_dir_len = math.hypot(AP_dir[0], AP_dir[1])
1407     AP_dir_unit = (AP_dir[0]/AP_dir_len, AP_dir[1]/AP_dir_len)
1408
1409     # Parametric line for AP: A + t * AP_dir_unit
1410     # Find intersection with circle with diameter AO
1411
1412     # Equation of circle with diameter AO
1413     # (x - mid_x)^2 + (y - mid_y)^2 = r^2
1414     mid_x = (A[0] + O[0])/2
1415     mid_y = (A[1] + O[1])/2
1416     r = AO / 2
1417
1418     # Parametric equations for line AP
1419     # x = A[0] + t * AP_dir_unit[0]
1420     # y = A[1] + t * AP_dir_unit[1]
1421
1422     # Substitute into circle equation
1423     # (x - mid_x)^2 + (y - mid_y)^2 = r^2
1424     # Expand and solve for t
1425
1426     def solve_for_t():
1427         # x = A[0] + t * dx
1428         # y = A[1] + t * dy
1429         dx = AP_dir_unit[0]
1430         dy = AP_dir_unit[1]
1431
1432         # Expand (x - mid_x)^2 + (y - mid_y)^2 = r^2
1433         # (A[0] + t*dx - mid_x)^2 + (A[1] + t*dy - mid_y)^2 = r^2
1434         # Expand terms
1435         a = dx**2 + dy**2
1436         b = 2 * (dx*(A[0] - mid_x) + dy*(A[1] - mid_y))
1437         c = (A[0] - mid_x)**2 + (A[1] - mid_y)**2 - r**2
1438
1439         # Solve a*t^2 + b*t + c = 0
1440         discriminant = b**2 - 4*a*c
1441         if discriminant < 0:
1442             return None
1443         t1 = (-b + math.sqrt(discriminant)) / (2*a)
1444         t2 = (-b - math.sqrt(discriminant)) / (2*a)
1445         return t1, t2
1446
1447         t_values = solve_for_t()
1448         if t_values:
1449             t = t_values[0] # Choose one solution, the other might be A itself
1450             px = A[0] + t * AP_dir_unit[0]
1451             py = A[1] + t * AP_dir_unit[1]
1452             P = (px, py)
1453         else:
1454             P = None
1455
1456         # Now compute perimeter of triangle BPC
1457         if P:
1458             def distance(p1, p2):
1459                 return math.hypot(p1[0]-p2[0], p1[1]-p2[1])
1460
1461             BP = distance(B, P)
1462             CP = distance(C, P)
1463             BC = distance(B, C)
1464             perimeter = BP + CP + BC
1465             print(perimeter)
1466         else:
1467             print("No intersection found")

```

1458

1459

130

1460

1461

&lt;/code&gt;

1462

&lt;interpreter&gt; 192.0 &lt;/interpreter&gt;

1463

The code computes the perimeter of triangle BPC and returns 192.0. Therefore, the answer is 192.

1464

1465

1466

1467

1468

1469

1470

1471

1472

1473

1474

1475

1476

1477

1478

1479

1480

1481

1482

1483

1484

1485

1486

1487

1488

1489

1490

1491

1492

1493

1494

1495

1496

1497

1498

1499

1500

1501

1502

1503

1504

1505

1506

1507

1508

1509

1510

1511